Multiplexed MPC for Multi-Zone Thermal Processing in Semiconductor Manufacturing

Andreas

A THESIS SUBMITTED
FOR THE DEGREE OF MASTER OF ENGINEERING

DEPARTMENT OF ELECTRICAL AND COMPUTER ENGINEERING
NATIONAL UNIVERSITY OF SINGAPORE

2008

Acknowledgements

I would like to express my gratitude to my supervisor, associate professor Ho Weng Khuen for his guidance through my M.Eng. study. Without his gracious encouragement and generous guidance, I would not be able to finish my work. His unwavering confidence and patience have aided me tremendously. I would like to extend special thanks to associate professor Ling Keck Voon. His wealth of knowledge and accurate foresight have greatly impressed and benefited me. I am indebted to him for his care and advice.

I would also like to express my thanks to my friends and colleagues, Mrs. Wu Bing Fang, Ms. Nandar Lyn, Mr. Yan Han, Mr. Feng Yong, Mr. Chen Ming and many others in the advanced control technology lab who have helped me a lot during my study. I would like to acknowledge the National University of Singapore and AUN SEED-Net for providing research facilities and financial support.

Finally, I want to thank my parents, without their support, I could never achieve this goal. I want to dedicate this thesis to my brother and sister and hope that they will enjoy it.

Contents

List of Figures

Summary

Photolithography process is regarded as the center and the most important process in semiconductor manufacturing due to its strong influence on cost and performance of a microchip. In the photolithography sequences, the most important variable to be controlled is critical dimension (CD) which is the minimum feature size dimension. One of major source of CD variation is the thermal processing in lithography, such as post-exposure bake (PEB) and post-apply bake. Thermal processing of semiconductor wafers is commonly performed by placement of the wafer on a heated plate for a given period of time. A general requirement for these systems is the ability to reject the load disturbance induced by placement of a cold wafer on the bake plate. Sluggish response can cause difficulties with, for example, repeatability of the manufacturing process if the recovery time of the temperature disturbance is longer than the baking time of the wafer and the next wafer comes before the temperature recovers.

Work on applications of model predictive control (MPC) as feedback controller for bake plate temperature control has been done experimentally in many papers. In a recent work, a variant of MPC called Multiplexed MPC, or MMPC, which claimed to have the potential for faster disturbance recovery response over the conventional MPC

was proposed. One characteristic of MPC is online optimization. Since optimization is conducted every sampling time, therefore computational power is likely an issue. All MPC theory to date and as far as we know the implementation, assume that all the control inputs are updated at the same instant or we called synchronized MPC (SMPC). In contrast, MMPC updates only one control input at a time. This will lead to suboptimal control signals. However, with reduced computational time, MMPC can use shorter update period, and updating all inputs one after another consecutively in the same period with SMPC.

In this thesis, we have designed MMPC feedback controller for bake plate temperature control and conduct the experiment to show the improvement from standard MPC controller. Since the model is important for MPC controller to work properly, we have conducted bake plate physical modeling and system identification. The computational advantage of MMPC becomes even more significant when constraints are considered and with increasing number of zones and control horizon.

Chapter 1

Introduction

1.1 Motivations

Semiconductor manufacturing has greatly affected the world due to the wide application of semiconductor devices. The industry development can basically be resembled by the so called integrated circuit (IC) scaling. The number of transistors on a single IC doubles in every two years according to Moore's law (Hamilton, 2003). Critical dimension (CD) of patterns is currently reduced below $100nm$. A more stringent demand on the CD variation is imposed. By the year 2010, a CD control requirement of $4.7nm$ is expected for $45nm$ technology node (*International Technology Roadmap for Semiconductors, 2005*). The industry has moved through several lithography generations to achieve smaller feature sizes. However, technology transition is expensive and time consuming. To reduce the cost a better way is to extend the life cycle of current lithography generation. The

challenge is to maintain CD variation within specifications while pushing feature size to its absolute minimum achievable value. One solution is the introduction of advanced equipment and process control (Moynes, 2006; Miyagi *et al.*, 2006).

According to Franssila (2004), Microfabrication processes consist of four basic operations which are high-temperature processes, thin-film deposition processes, patterning, layer transfer and bonding. Photolithography, a process which include some of these basic processes, is regarded as the center and the most important process due to its strong influence on cost and performance of a microchip. In the photolithography sequences, the most important variable to be controlled is critical dimension (CD) which is the minimum feature size dimension. CD is perhaps the single variable with the most impact on device speed and performance (Tay *et al.*, 2004; Edgar, 2000). The CD is significantly affected by several variables (Kim *et al.*, 2004). Exposure was regarded as an important source for CD variation (Postnikov *et al.,* 2003), and the errors may originate from exposure dose, grid size and illumination condition. Another major source of CD variation is the thermal processing in lithography, such as post-exposure bake (PEB) (Li, 2001; Cain *et al.,* 2005), and post-apply bake (Raptis, 2001).

Thermal processing of semiconductor wafers is commonly performed by placement of the wafer on a heated plate for a given period of time. The heated plate is of large thermal mass relative to the wafer and is held at a constant temperature by a feedback controller that adjusts the resistive heater power in response to a temperature sensor embedded in the plate near the surface. The plate is designed with multiple radial zone

configurations. The wafer may be placed in direct contact or on proximity pins. Processes that utilize this thermal approach include photoresist processing, chemical vapor deposition and rapid thermal annealing, and span a large temperature range (Campbell, 1996; Schaper *et al.*, 1994).

A general requirement for these systems is the ability to reject the load disturbance induced by placement of a cold wafer on the bake plate. Figure 1-1 shows the closed-loop temperature response of a bake plate used for photoresist processing when a $200mm$ wafer at a room temperature was placed on the bake plate. Initially the temperature dropped and then recovered because of closed-loop control. In manufacturing, wafers are processed in quick successions, one after another. Sluggish response can cause difficulties with, for example, repeatability of the manufacturing process if the recovery time of the temperature disturbance is longer than the baking time of the wafer and the next wafer comes before the temperature recovers. When this happens, there is not only wafer-to-wafer non-repeatability in temperature processing trajectory, but also plate-to-plate non-repeatability as the feedback controllers generally do not respond the same. If the processing temperature is not critical, then this type of response is acceptable. However, for some processes such as chemically amplified photoresist processing of the post-exposure bake step, temperature control is critical (Sturtevant *et al., 1993*; Pawlowski, 1997; ElAwady *et al.*, 1999).

Work on applications of model predictive control (MPC) as feedback controller for bake plate temperature control can be found in (Ho *et al.*, 2000; Lee *et al.*, 2002). In

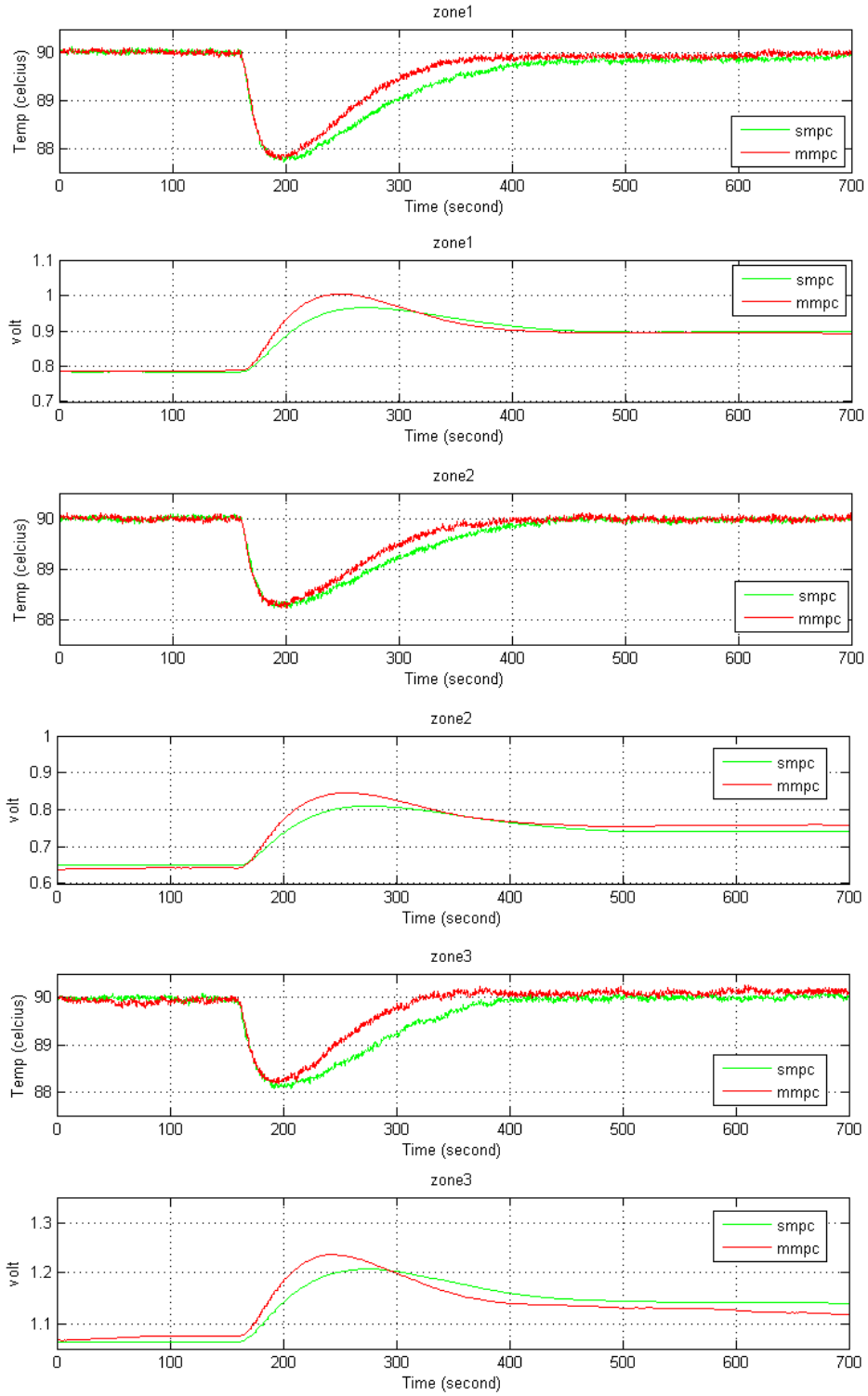

Figure 1-1: Close-loop experimental result using SMPC and MMPC controller for unconstrained case

addition, a linear quadratic gaussian (LQG) controller has been applied to a state-of-the-art 49-zone bake plate (Schaper *el al.*, 1999). LQG and MPC are optimal control strategies. In a recent work, a variant of MPC called Multiplexed MPC, or MMPC, which claimed to have the potential for faster disturbance recovery response over the conventional MPC was proposed (Ling *et al.*, 2005; Ling *et al.*, 2006). In this paper, we report the successful application of MMPC to improve the temperature recovery performance of a multi-zone bake plate. Figure 1-1 shows the improvement of MMPC over the standard MPC.

1.2 Contributions

In this thesis, both conventional MPC or *synchronized* MPC (SMPC) and multiplexed MPC (MMPC) controllers were designed for bake plate application. These feedback controllers will be used to maintain bake plate temperatures at set point 90^oC. The emphasis will be put on how MMPC performs compare to SMPC for disturbance rejection. Observation was made in the presence of disturbance caused by wafer placement on top of the bake plate at set point 90°C. This study has major contribution as the first experimental application of MMPC and support previous studies and simulation of MMPC (Ling *et al.*, 2005; Ling *et al.*, 2006; Ling *et al.*, 2008). The scope of this thesis covering bake plate modeling, SMPC and MMPC controllers design and its application in real experiment.

In the early part of this thesis, physical model of bake plate without wafer will be

derived using heat transfer law. Furthermore, system identification is conducted to get the true model for our specific bake plate. Using open loop experiment, we can observe the step response of the bake plate. Therefore, we can obtain model estimation by fitting experiment data into the structure of physical model we have derived. From experimental result, we have found that MMPC outperforms SMPC in term of recovery time after wafer with room temperature is dropped on top of the plate. However, we also found that MMPC is not as robust to white noise as SMPC. In the experiment, kalman filter was used to obtain the true states.

1.3 Organization

This thesis is organized as follow, Chapter 2 discuss plant modeling. In this chapter, a theoretical model of bake plate is constructed using heat transfer law. In Chapter 3, standard formulation of SMPC and MMPC problems is given for both finite and infinite horizon, constrained and unconstrained. In Chapter 4, the experimental setup is explained in details. To verify the accuracy of theoritical model, open loop system identification experiment is conducted. In this experiment, step input is given to one of the zones for every zone, then the step response result of open loop experiment and theoretical model simulation will be compared. The second part of this Chapter presents close-loop experimental result of the designed controller for bake plate temperatures control application with some discussion about the tuning. Finally Chapter 5 gives conclusions and recommendations for future work. Appendix A derives equivalent linear quadratic (LQ)

problem for SMPC to give fair basis for comparison with MMPC. Appendix B derives stabilizing terminal weight for infinite horizon MMPC.

Chapter 2

Bake Plate Thermal Modeling

The plant used in this project is a multi-zone bake plate which comprises of an aluminium plate with installed heaters at the bottom of the plate. Every heater is connected to input power so that it can heats up the plate according to the power given. The bake plate as shown in Figure 2-1 can be divided into multiple zones where each zone has its own separate heaters and every zone is powered separately. Between each zone there is $1mm$ air gap to reduce the effect of heat transfer between zones. A physical model of an m-zone bake plate has been derived in (Ho *et al.,* 2007) based on heat transfer laws. Because of the good heat conduction of metal, the temperature within each zone of bake plate is assumed to be sufficiently uniform. Thus a distributed lumped model can satisfactorily describe the plant characteristics. Heat transfer due to radiation can be safely neglected since its effect is small compared to conduction and convection at the temperature range of interest. Given the energy balance and heat transfer law, the bake plate can be modeled

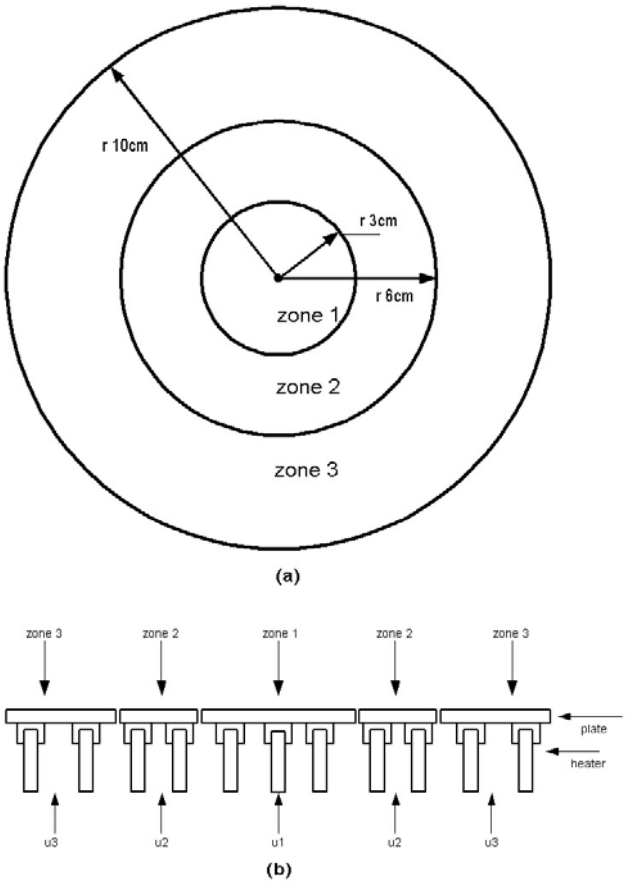

Figure 2-1: Diagram of bake plate. (a) top view; (b) side view

as

$$C_i\dot{T}_i(t) = p_i(t) + \frac{T_{(i-1)}(t) - T_i(t)}{r_{(i-1)i}} - \frac{T_i(t)}{r_i} + \frac{T_{i+1}(t) - T_i(t)}{r_{i(i+1)}} \tag{2.1}$$

where

$i =$ $1, 2, \cdots, m$ denotes zone i

$C_i =$ heat capacity of the ith zone (J/K)

$T_i(t) =$ The ith zone temperature above ambient (K)

$p_i =$ heater power to zone i (W)

$r_i =$ thermal resistance between zone i and surrounding air (K/W)

$r_{(i-1)i} =$ thermal resistance between zone $i-1$ and zone i; $r_{(i-1)i} = \infty$ for $i = 1$ (K/W)

$r_{i(i+1)} =$ thermal resistance between zone i and zone $i+1$; $r_{i(i+1)} = \infty$ for $i = m$ (K/W)

Assuming that ambient temperature is constant then at steady state $p_i(t) = p_i(\infty)$ and $T_i(t) = T_i(\infty)$, with $\dot{T}_i(\infty) = 0$, Eq. 2.1 can be formulated as

$$p_i(\infty) = -\frac{1}{r_{(i-1)i}}T_{i-1}(\infty) + \frac{1}{Ri}T_i(\infty) - \frac{1}{r_{i(i+1)}}T_{i+1}(\infty) \tag{2.2}$$

where R_i is the overall thermal resistance of zone i and can be calculated as

$$\frac{1}{R_i} = \frac{1}{r_i} + \frac{1}{r_{(i-1)i}} + \frac{1}{r_{i(i+1)}} \tag{2.3}$$

Because the baking process is not conducted at room temperature but at set point 90^oC, therefore it is easier if the variables used are relative temperatures with respect to the steady state temperatures rather than absolute temperatures. Defining new variables

$$\theta_i(t) = T_i(t) - T_i(\infty) \tag{2.4}$$

$$u_i(t) = p_i(t) - p_i(\infty) \tag{2.5}$$

Hence

$$T_i(t) = \theta_i(t) + T_i(\infty) \tag{2.6}$$

$$p_i(t) = u_i(t) + p_i(\infty) \tag{2.7}$$

$$\dot{\theta}_i(t) = \dot{T}_i(t) \tag{2.8}$$

$$\dot{u}_i(t) = \dot{p}_i(t) \tag{2.9}$$

Substituting Eq. 2.2, 2.3, 2.6 into Eq. 2.1 gives

$$C_i\dot{\theta}_i(t) = u_i(t) + \frac{1}{r_{(i-1)i}}\theta_{i-1}(t) + \frac{1}{r_{i(i+1)}}\theta_{i+1}(t) - \frac{1}{R_i}\theta_i \tag{2.10}$$

From Eq. 2.10 we can derive the state space model for a general m-zones bake plate in continuous time as

$$\dot{z} = A_c z + B_c u \tag{2.11}$$

$$y = C_c z$$

where

$$z = \begin{bmatrix} \theta_1 & \theta_2 & \cdots & \theta_m \end{bmatrix}^T$$

$$u = \begin{bmatrix} u_1 & u_2 & \cdots & u_m \end{bmatrix}^T$$

$$A_c = \begin{bmatrix} \frac{-1}{C_i R_i} & \frac{1}{C_i r_{12}} & & & 0 \\ \frac{1}{C_i r_{12}} & \frac{-1}{C_2 R_2} & \frac{1}{C_2 r_{23}} & & \\ & \frac{1}{C_3 r_{23}} & \frac{-1}{C_3 R3} & \ddots & \vdots \\ & & \ddots & \ddots & \frac{1}{C_{m-1}\, r_{(m-1)m}} \\ 0 & & & \frac{1}{C\, r_{(m-1)m}} & \frac{-1}{C_m R_m} \end{bmatrix}$$

$$B_c = \begin{bmatrix} \frac{1}{C_1} & & 0 \\ & \ddots & \\ 0 & & \frac{1}{C_m} \end{bmatrix}$$

$$C_c = \begin{bmatrix} 1 & & 0 \\ & \ddots & \\ 0 & & 1 \end{bmatrix} = I$$

Given the continuous-time model of Eq. 2.11, a discrete-time model, with discretization interval of h seconds, suitable for digital control design can be obtained as

$$\begin{aligned} z_{k+1} &= A_d z_k + B_d u_k \\ y_k &= C_d z_k \end{aligned} \tag{2.12}$$

where

$$A_d = e^{A_c h}, \qquad B_d = \int_0^h e^{A_c \tau} B_c d\tau, \qquad \text{and} \qquad C_d = C_c$$

Chapter 3

Controller Design

3.1 Introduction to Model Predictive Control (MPC)

Model predictive control (MPC) is a class of control algorithms which make explicit use of a model of the process to obtain the control signal by minimizing an objective function. The model is used to predict the process output at future time instant (horizon). Knowing these process output, a control sequence can be calculated to minimize the designed objective function. For each instant, this process is repeated and horizon is displaced toward the future. However, only the first control signal of the sequences is applied at each step, this is known as receding strategy. These three components are the main part of MPC. Acronym MPC denotes all types of predictive control laws, for which many other abbreviations exist such as GPC (Generalized Predictive Control), DMC (Dynamic Matrix Control), MAC (Model Algorithmic Control), PFC (Predictive Functional Control),

EPSAC (Extended Prediction Self Adaptive Control) and EHAC (Extended Horizon Adaptive Control) (Camacho and Bordons, 2004; Roberts, 2000). These various MPC algorithms only differ among themselves in the model used and cost function to be minimized. One of the most attractive features of MPC is that it can handle multivariable system naturally and can also handle input, output constraints explicitly by including them into problem formulation.

As is logical, however, MPC also has its drawbacks. One of these is that although the resulting control law is easy to implement and requires little computation, its derivation is more complex than that of classical PID controllers. The computation has to be carried out at every sampling time. When constraints are considered, the amount of computation required is even higher. Although this, with the computing power available today, is not an essential problem, one should bear in mind that many industrial process control computers are not at their best regarding their computing power. Another drawback is the need for an appropriate model of the process to be available. The design algorithm is based on prior knowledge of the model and is independent of it, but it is obvious that the benefit obtained will be affected by the discrepancies existing between the real process and the model used. However as long as the model is good enough for the purpose, one does not need to model all the physics, chemistry and internal behaviour of the process to get reliable model. The basic structure of MPC is depicted in Figure 3-1. All MPC theory to date and as far as we know the implementation, assume that all the control inputs are updated at the same instant (Maciejowski, 2002). Therefore, from this point

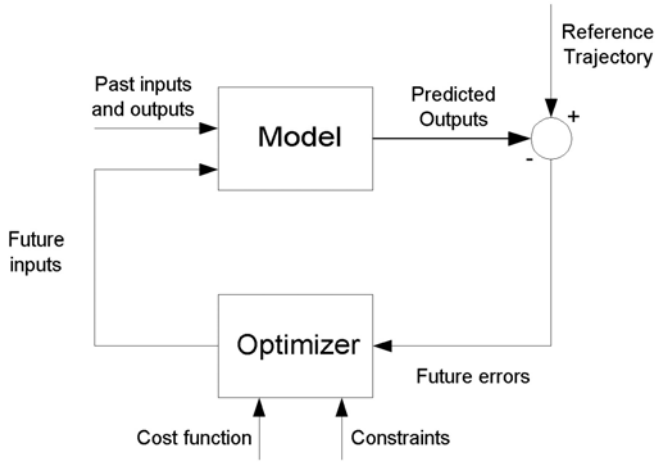

Figure 3-1: Basic structure of MPC

onward, this type of MPC will be identified as *synchronized* MPC (SMPC).

3.2 Synchronized Model Predictive Control (SMPC)

3.2.1 SMPC Model Formulation

For MPC design, it is more convenient to express the model (Eq. 2.12) with an incremental input, Δu, and one possibility is given below as

$$\begin{aligned} x_{k+1} &= Ax_k + B\Delta u_k \\ y_k &= Cx_k \end{aligned} \tag{3.1}$$

where

$$x_k = \begin{bmatrix} \Delta z_k \\ y_k \end{bmatrix}, \qquad A = \begin{bmatrix} A_d & 0 \\ C_d A_d & I \end{bmatrix}$$

$$B = \begin{bmatrix} B_d \\ C_d B_d \end{bmatrix}, \qquad C = \begin{bmatrix} 0 & C_d \end{bmatrix}$$

$$\Delta u_k = u_k - u_{k-1}, \qquad \Delta z_k = z_k - z_{k-1}$$

Using Δu as input instead of u has benefit for offset free tracking of constant set point since most of the time u is not zero when output y reaching set point w, but Δu is zero. It can also eliminates constant disturbance since the new augmented state contains Δx.

3.2.2 Prediction Model

We can predict the process output by iterating model 3.1.

$$\begin{aligned} y_{k+1} &= Cx_{k+1} \\ &= CAx_k + CB\Delta u_k \\ y_{k+2} &= Cx_{k+2} \\ &= CAx_{k+1} + CB\Delta u_{k+1} \\ &= CA^2x_k + CAB\Delta u_k + CB\Delta u_{k+1} \end{aligned}$$

or in general i-step ahead prediction of future output at current time instant k is

$$\begin{aligned} y_{k+i} &= Cx_{k+i} \\ &= CA^i x_k + \sum_{j=1}^{i} CA^{j-1} B \Delta u_{k+i-j} \end{aligned}$$

We can collect all the predicted outputs into a vector and arrange it as a prediction equation

$$\begin{bmatrix} y_{k+1} \\ y_{k+2} \\ \vdots \\ y_{k+N2} \end{bmatrix} = \underbrace{\begin{bmatrix} CA \\ CA^2 \\ \vdots \\ CA^{N2} \end{bmatrix}}_{past} x_k + \underbrace{\begin{bmatrix} CB & 0 & \cdots & 0 \\ CAB & CB & & \vdots \\ \vdots & & \ddots & \vdots \\ CA^{N2-1}B & CA^{N2-2}B & \cdots & CA^{N2-Nu}B \end{bmatrix} \begin{bmatrix} \Delta u_k \\ \Delta u_{k+1} \\ \vdots \\ \Delta u_{k+Nu-1} \end{bmatrix}}_{future}$$

Here, we are assuming there is no more change in the control input beyond the control horizon, i.e. $\Delta u_{k+i} = 0, \forall i \geq Nu$. Therefore we can obtain the following compact equation for output prediction

$$\vec{Y_k} = \Phi x_k + G\Delta\vec{U_k} \tag{3.2}$$

where

$$\begin{aligned}\vec{Y}_k &= \begin{bmatrix} y_{k+1} & y_{k+2} & \cdots & y_{k+N2} \end{bmatrix}^T \\ \Delta\vec{U}_k &= \begin{bmatrix} \Delta u_k & \Delta u_{k+1} & \cdots & \Delta u_{k+Nu-1} \end{bmatrix}^T\end{aligned}$$

3.2.3 Optimization Problem without Constraints

We can set SMPC cost function as

$$J = \sum_{i=0}^{N2} \|y_{k+i} - w_{k+i}\|_Q^2 + \sum_{i=1}^{Nu} \|\Delta u_{k+i-1}\|_R^2$$

This is standard cost function for set point tracking problem.

Note that $\vec{W}_k = \begin{bmatrix} w_{k+1}^T & w_{k+2}^T & \cdots & w_{k+N2}^T \end{bmatrix}^T$ is the vector of future set point. Therefore the optimization problem becomes

$$\begin{aligned} J &= (\vec{Y}_k - \vec{W}_k)^T Q(\vec{Y}_k - \vec{W}_k) + \Delta\vec{U}_k^T R\Delta\vec{U}_k \\ &= (\Phi + G\Delta\vec{U}_k - \vec{W}_k)^T Q(\Phi + G\Delta\vec{U}_k - \vec{W}_k) + \Delta\vec{U}_k^T R\Delta\vec{U}_k \\ &= \Delta\vec{U}_k^T (G^T QG + R)\Delta\vec{U}_k + 2\Delta\vec{U}_k^T G^T Q(\Phi x_k - \vec{W}_k) + const \end{aligned} \tag{3.3}$$

Minimizing Eq. 3.3 with respect to $\Delta\vec{U}_k$, we get a linear feedback control law:

$$\Delta\vec{U}_k = K_1\vec{W}_k + K_2 x_k$$

where

$$\begin{aligned} K_1 &= (G^T Q G + R)^{-1} G^T \\ K_2 &= -(G^T Q G + R)^{-1} G^T \Phi \end{aligned}$$

3.2.4 Constraints

Constraint is very important in system. In practice all processes are subject to some constraints. For example, actuator has physically limited field of action. Sometimes environmental and safety reasons tightened the limit such as maximum temperature or pressure. For most of the system there are three important constraints which normally should be put into consideration which are input constraints, input increment constraints, and output constraints. These constraints can be written as

$$\begin{aligned} u_{\min} &\leq u_{k+i} \leq u_{\max} \qquad i = 0, 1, \cdots, Nu - 1 \\ \Delta u_{\min} &\leq \Delta u_{k+i} \leq \Delta u_{\max} \qquad i = 0, 1, \cdots, Nu - 1 \\ y_{\min} &\leq y_{k+i} \leq y_{\max} \qquad i = 1, 2, \cdots, N2 \end{aligned}$$

We can arrange this equation to make it in standard form $\Omega \Delta \hat{U} \leq \omega$

For input increment constraints, we can formulate it as

$$\begin{aligned} -\Delta u_{k+i} &\leq -\Delta u_{\min} \\ \Delta \hat{u}_{k+i} &\leq \Delta u_{\max} \end{aligned}$$

or in general

$$\begin{bmatrix} -I \\ I \end{bmatrix} \Delta \vec{U}_k \leq \begin{bmatrix} -\Delta \vec{U}_{\min} \\ \Delta \vec{U}_{\max} \end{bmatrix}$$

For input constraints, it can be formulated as

$$\begin{bmatrix} u_k \\ u_{k+1} \\ \vdots \\ u_{k+Nu-1} \end{bmatrix} = \underbrace{\begin{bmatrix} I & 0 & 0 & 0 \\ I & I & 0 & 0 \\ \vdots & \ddots & \ddots & \vdots \\ I & \cdots & \cdots & I \end{bmatrix}}_{Eu} \begin{bmatrix} \Delta u_k \\ \Delta u_{k+1} \\ \vdots \\ \Delta u_{k+Nu-1} \end{bmatrix} + \underbrace{\begin{bmatrix} I \\ I \\ I \\ I \end{bmatrix}}_{\Upsilon} u_{k-1}$$

or in standard form

$$\begin{bmatrix} -Eu \\ Eu \end{bmatrix} \Delta \vec{U}_k \leq \begin{bmatrix} -(\vec{U}_{\min} - \Upsilon u_{k-1}) \\ \vec{U}_{\max} - \Upsilon u_{k-1} \end{bmatrix}$$

where

$$\vec{U}_{\min} = \begin{bmatrix} u_{\min}^T & u_{\min}^T & \cdots & u_{\min}^T \end{bmatrix}^T$$

$$\vec{U}_{\max} = \begin{bmatrix} u_{\max}^T & u_{\max}^T & \cdots & u_{\max}^T \end{bmatrix}^T$$

For output constraints, the formulation is

$$\begin{aligned} \vec{Y}_k &= \Phi x_k + G\Delta\vec{U}_k \\ \vec{Y}_{\min} - \Phi x_k &\leq G\Delta\vec{U}_k \leq \vec{Y}_{\max} - \Phi x_k \end{aligned}$$

Hence

$$\begin{bmatrix} -G \\ G \end{bmatrix} \Delta\vec{U}_k \leq \begin{bmatrix} -(\vec{Y}_{\min} - \Phi x_k) \\ \vec{Y}_{\max} - \Phi x_k \end{bmatrix}$$

To make it more explicit we can combine all inequalities together into a single set

$$\Omega\Delta\vec{U}_k \leq \beta + \Gamma \begin{bmatrix} x_k \\ u_{k-1} \end{bmatrix} \tag{3.4}$$

where

$$\Omega = \begin{bmatrix} -I \\ -Eu \\ -G \\ I \\ Eu \\ G \end{bmatrix} \qquad \beta = \begin{bmatrix} -\Delta\vec{U}_{\min} \\ -\vec{U}_{\min} \\ -\vec{Y}_{\min} \\ \Delta\vec{U}_{\max} \\ \vec{U}_{\max} \\ \vec{Y}_{\max} \end{bmatrix} \qquad \Gamma = \begin{bmatrix} 0 & 0 \\ 0 & \Upsilon \\ \Phi & 0 \\ 0 & 0 \\ 0 & -\Upsilon \\ -\Phi & 0 \end{bmatrix}$$

Ω is time invariant. We only need to compose matrix Ω, β, Γonce and use it for every optimization since constraints are constant. As we can see from 3.4, there are very large inequalities involved even with small Nu and $N2$. For system with m inputs and p

outputs, the number of inequalities will be $2(2mNu + pN2)$.

3.2.5 Optimization Problem with Constraints

The optimization problem with constraints can be formulated as

$$\min J = \Delta\vec{U}_k^T(G^TQG + R)\Delta\vec{U}_k + 2\Delta\vec{U}_k^TG^TQ(\Phi x_k - \vec{W}_k) + const$$

subject to

$$\Omega\Delta\vec{U}_k \leq \beta + \Gamma \begin{bmatrix} x_k \\ \\ u_{k-1} \end{bmatrix}$$

This is a standard quadratic programming (QP) problem, where computation complexity depends on two parameters, number of decision variables and number of inequalities. This setup of cost function is known as finite horizon SMPC. There is no guarantee for nominal stability for this kind of setup. Even though one can change SMPC parameters such as horizon and weight to find appropriate tuning for a system. A more generic solution is to make use of infinite horizon by setting $Nu = N2 = N = \infty$ in cost function.

3.2.6 Infinite Horizon

It has been known that making the horizon infinite in predictive control will lead to guaranteed stability (Bitmead *et al.*, 1990). However, problem arises when constraints are involved because it is impossible to solve optimization problems with infinite variable to be solved. Muske and Rawlings (1993a, 1993b, 1995) have made some works to solve

this problem. The idea is to re-parameterize the predictive control problem with infinite horizon in term of finite number of parameters, so optimization can still be performed. One realization of infinite horizon is to compose it in two separated modes. Mode 1 is similar with previous finite horizon problem, while mode 2 use fixed linear control law to solve optimization problem beyond the horizon. To illustrate how it works, regulator problem will be used as example.

The cost function for regulator problem is

$$J = \sum_{i=0}^{\infty} (\|x_{k+i+1}\|_Q^2 + \|\Delta u_{k+i}\|_R^2)$$

We can separate it into two parts where $J = J_1 + J_2$

$$\begin{aligned} J_1 &= \sum_{i=0}^{N-1} (\|x_{k+i+1}\|_Q^2 + \|\Delta u_{k+i}\|_R^2) \\ J_2 &= \sum_{i=0}^{\infty} (\|x_{k+N+i+1}\|_Q^2 + \|\Delta u_{k+N+i}\|_R^2) \end{aligned}$$

Optimization problem for J_1 can be constructed using finite horizon method. Since

$$\vec{X}_k = \Psi x_k + \Theta \Delta \vec{U}_k, \qquad \vec{X}_k = \begin{bmatrix} x_{k+1}^T & x_{k+2}^T & \cdots & x_{k+N}^T \end{bmatrix}^T$$

where

$$\Psi = \begin{bmatrix} A \\ A^2 \\ \vdots \\ A^N \end{bmatrix}, \qquad \Theta = \begin{bmatrix} B & 0 & \cdots & 0 \\ AB & B & \cdots & 0 \\ \vdots & \ddots & \ddots & \vdots \\ A^{N-1}B & \cdots & \cdots & B \end{bmatrix} \tag{3.5}$$

therefore

$$J_1 = (\Psi x_k + \Theta \Delta \vec{U}_k)^T Q (\Psi x_k + \Theta \Delta \vec{U}_k) + \Delta \vec{U}_k^T R \Delta \vec{U}_k$$

For mode 2, we can define control law as

$$\Delta u_{k+i} = -K x_{k+i} \qquad for \;\; i \geq N$$

$$\begin{aligned} x_{k+i+N+1} &= (A - BK)\, x_{k+i+N} = \Phi x_{k+i+N} = \Phi^{i+1} x_{k+N} \qquad for \;\; i \geq 0 \\ \Delta u_{k+i+N} &= -K x_{k+i+N} = -K \Phi^i x_{k+N} \end{aligned}$$

so that

$$\begin{aligned} J_2 &= \sum_{i=0}^{\infty} x_{k+N}^T (\Phi^{i+1})^T Q \Phi^{i+1} x_{k+N} + x_{k+N}^T (-K\Phi^i)^T R (-K\Phi^i) x_{k+N} \\ &= \sum_{i=0}^{\infty} x_{k+N}^T [(\Phi^{i+1})^T Q \Phi^{i+1} + (\Phi^i)^T K^T R K \Phi^i] x_{k+N} \\ &= x_{k+N}^T P x_{k+N} \end{aligned}$$

where

$$P = \sum_{i=0}^{\infty} (\Phi^{i+1})^T Q \Phi^{i+1} + (\Phi^i)^T K^T R K \Phi^i$$

P can be solved using Lyapunov equation such that

$$\Phi^T P \Phi = P - \Phi^T Q \Phi - K^T R K$$

Since

$$x_{k+N} = \Psi_N x_k + \Theta_N \Delta \vec{U}_k$$

where $\Psi_N = A^N$ and $\Theta_N = \begin{bmatrix} AB^{N-1} & AB^{N-2} & \dots & B \end{bmatrix}$, therefore

$$J_2 = (\Psi_N x_k + \Theta_N \Delta \vec{U}_k)^T P (\Psi_N x_k + \Theta_N \Delta \vec{U}_k)$$

Combining J_1 and J_2, the cost function for infinite horizon MPC is

$$J = \Delta \vec{U}_k^T S_u \Delta \vec{U}_k + \Delta \vec{U}_k^T S_x x_k + const$$

where

$$\begin{aligned} S_u &= \Theta^T Q \Theta + R + \Theta_N^T P \Theta_N \\ S_x &= 2(\Theta^T Q \Psi + \Theta_N^T P \Psi_N) \end{aligned}$$

Note that the constraints handling assumes that the given fixed feedback law ensures

that beyond N the constraints are always satisfied.

3.2.7 SMPC Design for 3-zones Bake Plate

We will design infinite horizon SMPC controller for the bake plate model. From our original state space model

$$\begin{aligned} z_{k+1} &= A_d z_k + B_d u_k \\ y_k &= C_d z_k \end{aligned}$$

we can create new state space model with augmented states as

$$x_{k+1} = \begin{bmatrix} A_d & 0 \\ C_d A_d & I \end{bmatrix} x_k + \begin{bmatrix} B_d \\ C_d B_d \end{bmatrix} \Delta u_k$$

where

$$x_k = \begin{bmatrix} \Delta z_{1,k} \\ \Delta z_{2,k} \\ \Delta z_{3,k} \\ y_{1,k} - w_1 \\ y_{2,k} - w_2 \\ y_{3,k} - w_3 \end{bmatrix}$$

Instead of using y, we can substract the set point from the output $(y - w)$ and change it into regulator problem, so that control signal can be computed using methods we have

derived so far. Figure 3-2 shows step by step how to design SMPC controller. Prediction model matrix and constraints matrix are composed according to Eq. 3.5 and Eq. 3.4. We can put the infinite horizon weight or end point weighting P, obtained from LQR solution, as the last part of state weighting matrix Q and solve the optimization using quadratic programming (QP). For unconstrained case, SMPC solution is linear control law.

3.3 Multiplexed Model Predictive Control (MMPC)

As we know, one characteristic of MPC is online optimization. Since optimization is conducted every sampling time, therefore computational power is likely an issue especially in a system with lack of resources. If there is not enough time to compute the control signal before next sampling instant due to complexity of the problem then the controller will crash since there is not enough memory available to start new optimization while previous optimization still running. Or even worse, it will give wrong control signals since the plant demands inputs from controller. Therefore, it is important to find a way to reduce the computational time needed by MPC controller to calculate the control signals.

All MPC methods to date, require all input channels to be updated simultaneously. The way of traditional MPC became very big burden with the increase of the input number. Theory states that computational complexity including time requirement tend to vary as $O(m^3)$, where m is the number of control inputs. Multiplexed model predictive control (MMPC) tries to exploit this weakness of traditional MPC by updating only one

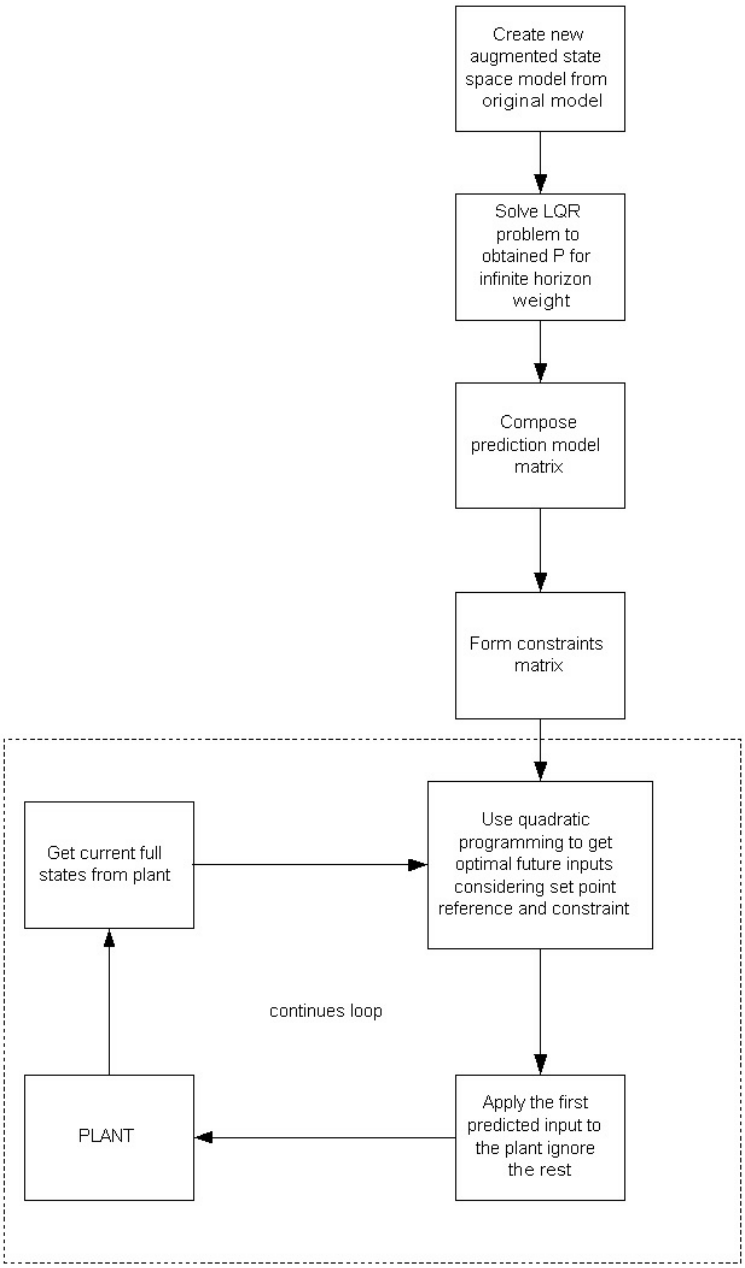

Figure 3-2: Flowchart of SMPC controller design

channel at a time instead of all channels. Off course, this will lead to suboptimal control signals. However, with reduced computational time, MMPC can use shorter update period, and updating all channels one after another consecutively in the same period with traditional MPC. This is why MMPC called multiplexed MPC. Here, we assume that fresh measurement of plant states are available at reduced sampling period. In many cases, it is better to response faster albeit suboptimal than optimal but very late. One example is in disturbance rejection case. Figure 3-3 shows the pattern of input update in the MMPC scheme with $m = 3$ compare to conventional MPC which updates all input simultaneously or we called *synchronized* MPC (SMPC).

MMPC scheme which updates all inputs "not" simultaneously really suit industrial practice since complex plant usually has large number of input to control and limited communication channel between controller and actuators so that it is impossible to update all control input simultaneously. One should note that there are many possible variation of MMPC scheme regarding its input pattern update. Sometimes, it is more useful to update one subset instead of only one input, or not to update all the inputs but decide in real time which one is more important to be updated more frequent. This variation of MMPC resembles statistical process control (SPC), which is used widely in manufacturing processes (Box and Luceno, 1997).

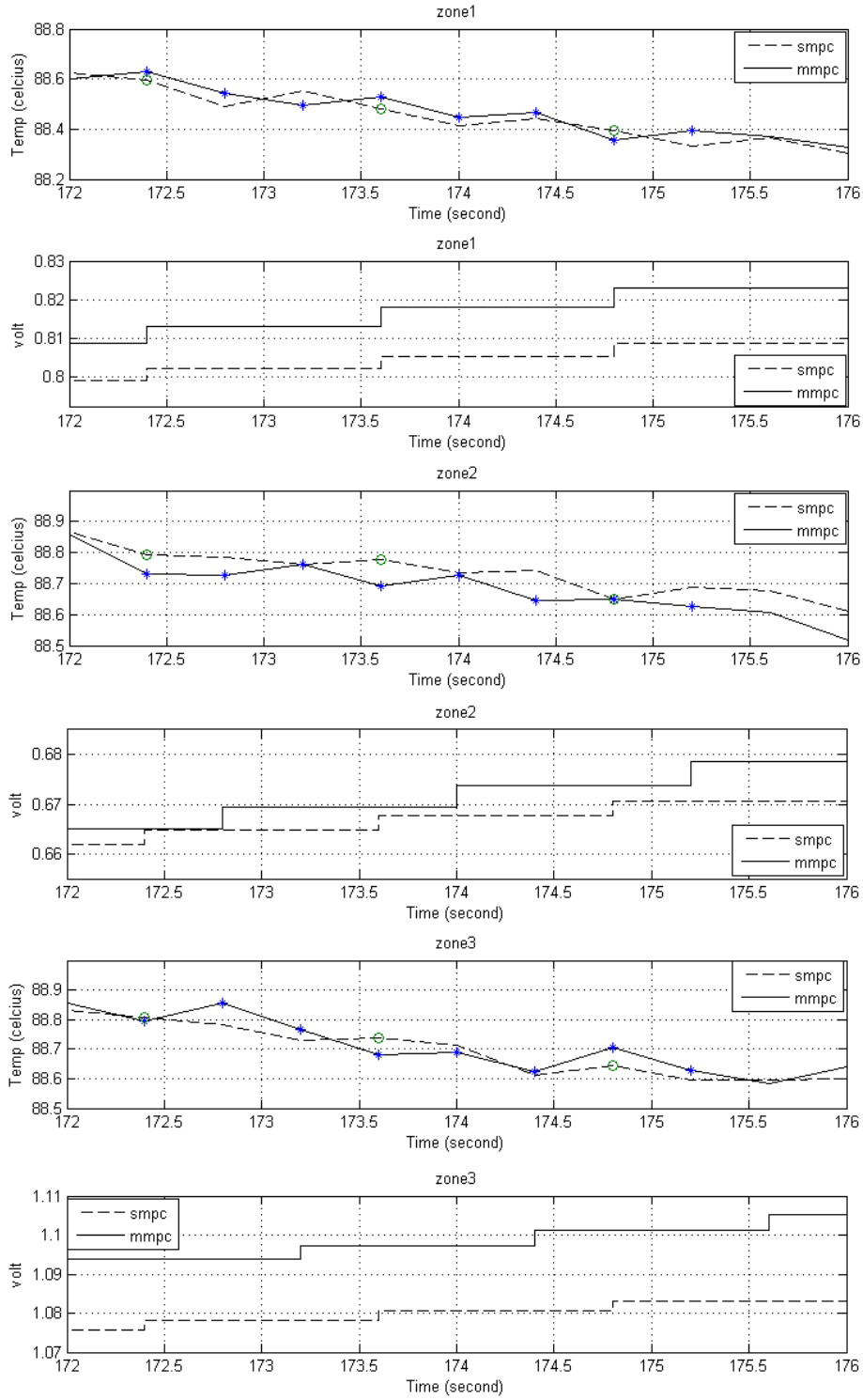

Figure 3-3: Pattern of inputs update for traditional or synchronized MPC (dashed line) and for multiplexed MPC (solid line)

3.3.1 Problem Formulation

Consider a discrete time linear state space model with state vector $x_k \in R^n$ and m inputs $u_{1,k}, \ldots, u_{m,k}$

$$x_{k+1} = Ax_k + \sum_{j=1}^{m} B_j \Delta u_{j,k} \tag{3.6}$$

where B_j is a column vector, $B_j \in R^{nxp_j}$ and $\Delta u_{j,k} = u_{j,k} - u_{j,k-1}$, $\Delta u_{j,k} \in R^{p_j}$, with $\sum_j p_j$ inputs.

We assume that $(A, [B_1, \ldots, B_m])$ is stabilizable. In this model k corresponds to a time duration T/m where T is the complete update cycle duration. Using this time index, we assume that at every time step k the complete states vector x_k is known from measurement. Now we can introduce the indexing function,

$$\sigma(k) = (k \bmod m) + 1 \tag{3.7}$$

$\sigma(k)$ indicates what input channel we are updating at a time. As we can see from Eq. 3.7 the value of $\sigma(k)$ will reset after the last input channel. We use the model in Eq. 3.6 because MMPC updating only one input at a time so that at one time only one Δu has a value, the rest are zero. However, after one complete update cycle T all of the inputs are updated.

$$\Delta u_{j,k+i} = 0 \; if \; j \neq \sigma(k+i)$$

Alternatively, we can also represent model 3.6 as periodic linear system

$$x_{k+1} = Ax_k + B_{\sigma(k)}\Delta\tilde{u}_k \tag{3.8}$$

where $\Delta\tilde{u}_k = \Delta u_{\sigma(k),k}$ and $B_{\sigma(k)}$ is column vector of B matrix. Which column it refers to is indicated by column index $\sigma(k)$.

Unlike the original model, this periodic linear system (3.8) has different model for different time, it has exactly m model which will be used one after another and will be repeated after one complete update cycle. This model assumes that only one input is updated at a time. It is more explicit and more convenient to represent the model this way, therefore this representation will be used from this point onward. Using similar procedure with SMPC the N-step prediction model for MMPC is

$$\vec{X}_{k+1} = \phi x_k + G_{\sigma(k)}\Delta\vec{U}_k$$

where

$$\vec{X}_{k+1} = \begin{bmatrix} x_{k+1} \\ x_{k+2} \\ \vdots \\ x_{k+N} \end{bmatrix}, \qquad \Delta\vec{U}_k = \begin{bmatrix} \Delta\tilde{u}_k \\ \Delta\tilde{u}_{k+1} \\ \vdots \\ \Delta\tilde{u}_{k+N-1} \end{bmatrix}$$

$$\phi = \begin{bmatrix} A \\ A^2 \\ \vdots \\ A^N \end{bmatrix}, \qquad G_{\sigma(k)} = \begin{bmatrix} B_{\sigma(k)} & 0 & \cdots & 0 \\ AB_{\sigma(k)} & B_{\sigma(k+1)} & \cdots & 0 \\ \vdots & \ddots & \ddots & \vdots \\ A^{N-1}B_{\sigma(k)} & \cdots & AB_{\sigma(k+N-2)} & B_{\sigma(k+N-1)} \end{bmatrix}$$

Let $N = (Nu-1)m+1$ where Nu is the control horizon, a parameter which indicates the number of control moves to be optimized per input channel. Then we can write the prediction model into different form by grouping the control signals into m vectors as follows:

$$\vec{X}_{k+1} = \phi x_k + g_1^{\sigma(k)}\Delta\vec{u}_{k,0} + g_2^{\sigma(k)}\Delta\vec{u}_{k,1} + \ldots + g_m^{\sigma(k)}\Delta\vec{u}_{k,m-1}$$

where

$$\Delta\vec{u}_{k,0} = \begin{bmatrix} \Delta\tilde{u}_k \\ \Delta\tilde{u}_{k+m} \\ \vdots \\ \Delta\tilde{u}_{k+(Nu-1)m} \end{bmatrix}$$

$$\Delta\vec{u}_{k,i} = \begin{bmatrix} \Delta\tilde{u}_{k+i} \\ \Delta\tilde{u}_{k+m+i} \\ \vdots \\ \Delta\tilde{u}_{k+(Nu-2)m+i} \end{bmatrix}$$

for $i = 1, 2, \ldots, m-1$ and $g_i^{\sigma(k)}$ $i = 1, 2, \ldots, m$ are matrices whose columns are columns of

the $G_{\sigma(k)}$ matrix, namely, $g_1^{\sigma(k)}$ is the matrix whose columns are columns $1, 1+m, \ldots, 1+(Nu-1)m$ of the $G_{\sigma(k)}$, while $g_i^{\sigma(k)}$ $i = 2, \ldots, m$ contains columns $i, i+m, \ldots, i+(Nu-2)m$ columns of $G_{\sigma(k)}$.

In this MMPC scheme, we only do optimization for one input channel of system. Assumption were made for other input channels. Therefore, at time k except for active channel (active channel refer to input channel which will be optimized at time k) we will use the result of optimized control signals from previous optimization process at time $k-1, k-2, \ldots, k-m-1$ for the cost function. It has been explained in Chapter 3.2 that SMPC uses only the first control signal from Nu numbers of computed control signal and throws away the rest. By using this "wasted computed control signal" for next optimization, MMPC can reduce computational time greatly. At time k we assume that previous predicted control signal from other channels that has been computed but not executed are true and eventually will be executed as planned, even though in practice this assumption usually not true since new measurement give us more recent condition of plant. This prediction inaccuracy will lead to suboptimality of MMPC. However, it is often the case that reacts sooner albeit suboptimal leads to better control than reacts optimally but later. Actually, there is another MMPC scheme (Ling *et al.*, 2006) which updates one input at a time but compute optimal control signal for all channels every time step k. Since the number of decision variables is the same with SMPC, there is no computational reduction using this scheme. Because of no practical interest for this scheme therefore we will exclude the explanation from this thesis. The MMPC scheme

acquires more information than SMPC and distributes the control moves over a complete update cycle. Thus, the multiplexed MPC solves the following finite-time constrained linear periodic control problem

$$
\begin{aligned}
& P_{\sigma(k)}(x_k) : \min J_k = F(x_{k+N|k}) + \textstyle\sum_{i=0}^{N-1} (\left\|x_{k+i+1|k}\right\|_q^2 + \left\|\Delta\tilde{u}_{k+i|k}\right\|_r^2) \\
& wrt \qquad \Delta\tilde{u}_{k+i|k}, \qquad (i = 0, m, 2m, \ldots, N-1) \\
& s.t. \qquad \Delta\tilde{u}_{k+i|k} \in U, \qquad (i = 0, 1, \ldots, N-1) \\
& \qquad\quad x_{k+i|k} \in X, \qquad (i = 1, \ldots, N) \\
& \qquad\quad x_{k+N+1|k} \in \chi_I(K_{\sigma(k)}) \\
& \qquad\quad x_{k+1|k} = Ax_{k|k} + B_{\sigma(k)}\Delta\tilde{u}_{k|k} \\
& \qquad\quad \Delta\tilde{u}_{k+i|k} = \Delta\tilde{u}_{k+i|k-1}, \qquad \forall i \neq jm
\end{aligned}
$$

where $q = q^T > 0,\ r = r^T \geq 0$ and $F(x_{k+N|k})$ is suitably chosen terminal cost. X and U are compact polyhedral sets containing the origin in their interior. $\chi_I(K_{\sigma(k)})$ denotes the sets in which none of the constraints is active, and which is the maximum positively invariant set (Blanchini, 1999) for the linear periodic system (3.8), when a stabilizing linear periodic feedback controller $K_{\sigma(k)}$ is applied, namely

$$x_k \in \chi_I(K_{\sigma(k)}) \Longrightarrow K_{\sigma(k)} \in U \quad \text{and}$$

$$(A + B_{\sigma(k)}K_{\sigma(k)})x_k \in \chi_I(K_{\sigma(k)})$$

where $\chi_I(K_{\sigma(k)}) \subset X$.

We can imagine MMPC scheme as m MPC controllers, operating in sequence, in cyclic manners. They share informations, however, in the sense that the complete plant states is available to each controller, although not at the same time, and the currently planned future moves of each controller are also available to all the others. Constraints for MMPC can be formulated following the same procedure with SMPC.

3.3.2 MMPC Design for 3-zones Bake Plate

Design of MMPC controller can be made following the same procedure with SMPC. The only different is MMPC send unused predicted control signal for next optimization as can be seen in Figure 3-4. The model used in MMPC will be different for different input channels. Therefore every input channels has their own terminal weighting and prediction model matrix. For implementation, we will use the following state space to help us obtain appropriate control signals from other channels.

$$\Delta\vec{u}_{k+1} = A_u\Delta\vec{u}_k + B_u\Delta\vec{u}_k \tag{3.9}$$

where

$$\Delta\vec{u}_{k+1} = \begin{bmatrix} \Delta\bar{u}_{k-m+2} \\ \Delta\bar{u}_{k-m+3} \\ \vdots \\ \Delta\bar{u}_{k-1} \\ \Delta\bar{u}_k \end{bmatrix}, \qquad \Delta\vec{u}_k = \begin{bmatrix} \Delta\bar{u}_{k-m+1} \\ \Delta\bar{u}_{k-m+2} \\ \vdots \\ \Delta\bar{u}_{k-2} \\ \Delta\bar{u}_{k-1} \end{bmatrix}$$

$$\Delta\bar{u}_k = \begin{bmatrix} \Delta u_{k+m} \\ \Delta u_{k+2m} \\ \vdots \\ \Delta u_{k+(Nu-1)m} \end{bmatrix}$$

$$A_u = \begin{bmatrix} 0 & I & 0 & \cdots & 0 \\ 0 & 0 & I & & 0 \\ \vdots & & \ddots & \ddots & \vdots \\ \vdots & & \ddots & \ddots & \vdots \\ 0 & \cdots & \cdots & \cdots & 0 \end{bmatrix}, \qquad B_u = \begin{bmatrix} 0 \\ 0 \\ \vdots \\ \vdots \\ I \end{bmatrix}$$

After every optimization finished first control signal will be sent to actuator, and the rest of predicted control signal will be fed into state space 3.9 as inputs. At next optimization process, the outputs of the state space will be taken as predicted control signal from other channels. This process is repeated continuously during implementation of MMPC controller.

3.4 Kalman Filter

To get the true states from noise distorted output measurement, we need to do state estimation. This can be done using kalman filter as states observer. Discrete kalman filter has two components which are time update and measurement update. Consider a

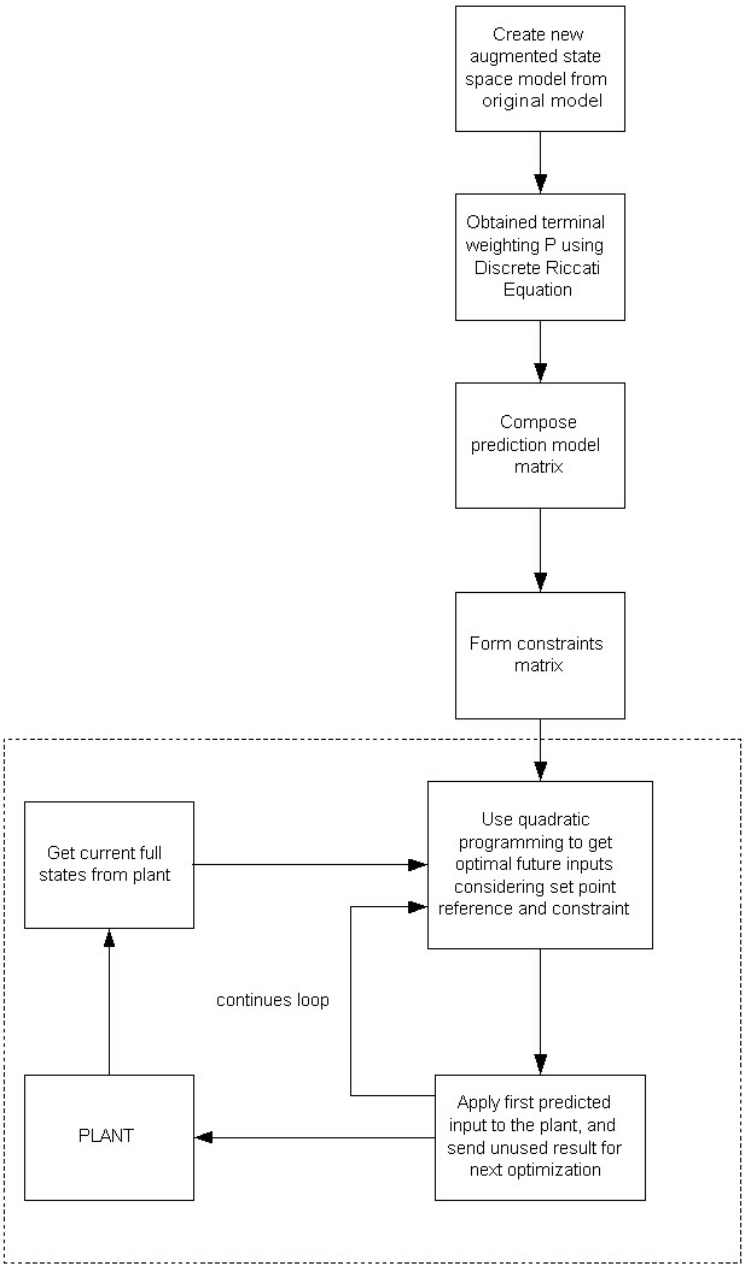

Figure 3-4: Flowchart of MMPC controller design

discrete state space model

$$\begin{aligned} z_{k+1} &= A_d z_k + B u_k + G w_k \\ y_k &= C_d z_k + v_k \end{aligned} \tag{3.10}$$

where w_k and v_k are process and measurement noise.

Please note that (3.10) is the original state space model not the augmented state space model.

$$\begin{aligned} z_{k+1|k} &= A_d z_{k|k-1} + B_d u_k + A_d M(y_k - C_d z_{k|k-1}) \\ &\underbrace{= A_d(I - MC_d) z_{k|k-1} + \begin{bmatrix} B_d & A_d M \end{bmatrix} \begin{bmatrix} u_k \\ \\ y_k \end{bmatrix}}_{\text{Time Update}} \end{aligned}$$

$$\begin{aligned} z_{k|k} &= z_{k|k-1} + M(y_k - C_d z_{k|k-1}) \\ &\underbrace{= (I - MC_d) z_{k|k-1} + M y_k}_{\text{Measurement Update}} \end{aligned}$$

where M is innovation gain.

To make it easier in implementation, we can further arrange the equation

$$\begin{aligned} z_{k+1|k} &= A_d z_{k|k-1} + B_d u_k + A_d M(y_k - C_d z_{k|k-1}) \\ &= A_d z_{k|k-1} - A_d M C_d z_{k|k-1} + A_d M y_k + B_d u_k \\ &= A_d(z_{k|k-1} + M(y_k - C_d z_{k|k-1})) + B_d u_k \\ &= A_d z_{k|k} + B_d u_k \end{aligned} \tag{3.11}$$

Backshift Eq. 3.11,

$$z_{k|k-1} = A_d z_{k-1|k-1} + B_d u_{k-1}$$

Then substitute it into the measurement update equation

$$\begin{aligned} z_{k|k} &= (I - MC_d) z_{k|k-1} + M y_k \\ &= (I - MC_d)(A_d z_{k-1|k-1} + B_d u_{k-1}) + M y_k \\ &= (I - MC_d) A_d z_{k-1|k-1} + (I - MC_d) B_d u_{k-1} + M y_k \\ &= (I - MC_d) A_d z_{k-1|k-1} + \begin{bmatrix} (I - MC_d) B_d & M \end{bmatrix} \begin{bmatrix} u_{k-1} \\ y_k \end{bmatrix} \end{aligned} \tag{3.12}$$

Equation 3.12 is the discrete kalman filter state space. To get the states estimation we need current output measurement y_k and previous input u_{k-1}.

Chapter 4

Experimental Result

4.1 Experimental Setup

The experimental setup consists of four parts, which are PC with LabVIEW, silicon rectified controller (SCR) power controller, data acquisition card (DAQ), and multi-zone bake plate (see Figure 4-1 and Figure 4-2). SCR type Watlow Dynamite power controllers model DC 1P-5012-V100 are used in this experiment (Watlow, 1995). SMPC and MMPC controllers are designed in LabVIEW environment. After optimal control signals are found, they will be sent to the power controllers and heat up arrangement of heaters under the plate. Experimental setup diagram is shown in Figure 4-3. An array of temperature sensor elements are embedded on top of the heaters to read the plate temperatures and send the signals to the PC through data acquisition card (DAQ). The bake plate can be easily configured into multiple zones depend on the application. In

Figure 4-1: Top view photograph of multizone bake plate

Figure 4-2: Side view photograph of multizone bake plate

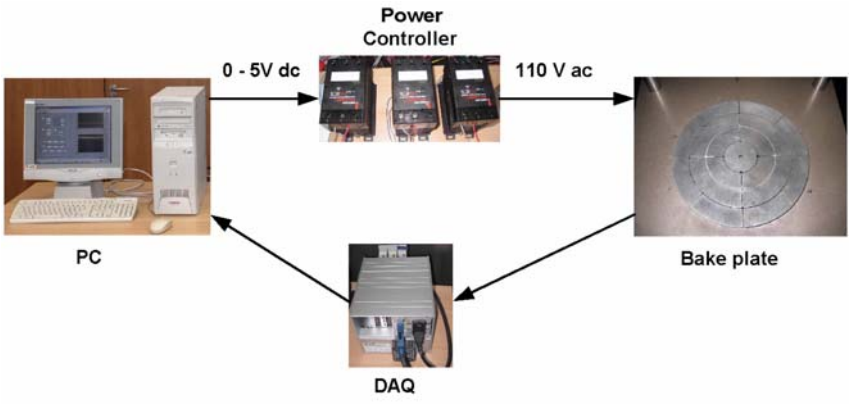

Figure 4-3: Experimental setup diagram

this project, the bake plate is configured into three zones as shown in Figure 2-1. After temperature of all zones reach the set point 90^oC, $200mm$ wafer with room temperature will be dropped on top of the plate. Proximity pins are placed on top of the plate to avoid direct contact between wafer and plate surface. This will create an air gap approximately $165\mu m$ between wafer and plate.

4.2 System Identification

The physical model derived in Section 2 suggests a particular structure for the state space matrices. Given this structure, we used the System Identification Toolbox from MATLAB to perform a structured state-space model estimation to estimate its unknown parameters.

Open loop step response tests were carried out to collect the required input-output data for parameter estimation. First, the temperatures of all zones were made to reach

steady state of around 90^oC (baking process temperature). In this experiment the steady state input voltages are $0.86V, 0.75V$, and $1.14V$ for zone 1, zone 2, and zone 3 consecutively. The steady state temperatures at those voltages are 89.5^oC (zone 1), 89.6^oC (zone 2), and 89.5^oC (zone 3). Then a step input of magnitude $0.3V$ was applied to the heaters of one zone while inputs to the other two remaining heater zones were maintained constant. The temperature changes in all three zones were recorded. This process was repeated for the other two inputs.

The relationship between given input voltage and output temperature for each zone are shown in Figure 4-4 where the y-axis shows the value of plate temperature after substracting the steady state temperature. In this experiment we use sampling time $1s$. As we expected there are some heat transfer between each zones.

The result of the parametric model estimation is given below :

$$A_c = \begin{bmatrix} -0.0025525 & 0.0019085 & 0 \\ 0.0007048 & -0.004652 & 0.003324 \\ 0 & 0.0030697 & -0.004471 \end{bmatrix}$$

$$B_c = \begin{bmatrix} 0.0052573 & 0 & 0 \\ 0 & 0.0019416 & 0 \\ 0 & 0 & 0.0017926 \end{bmatrix}$$

Evaluating parameters of structured physical model we have derived before, we can obtain

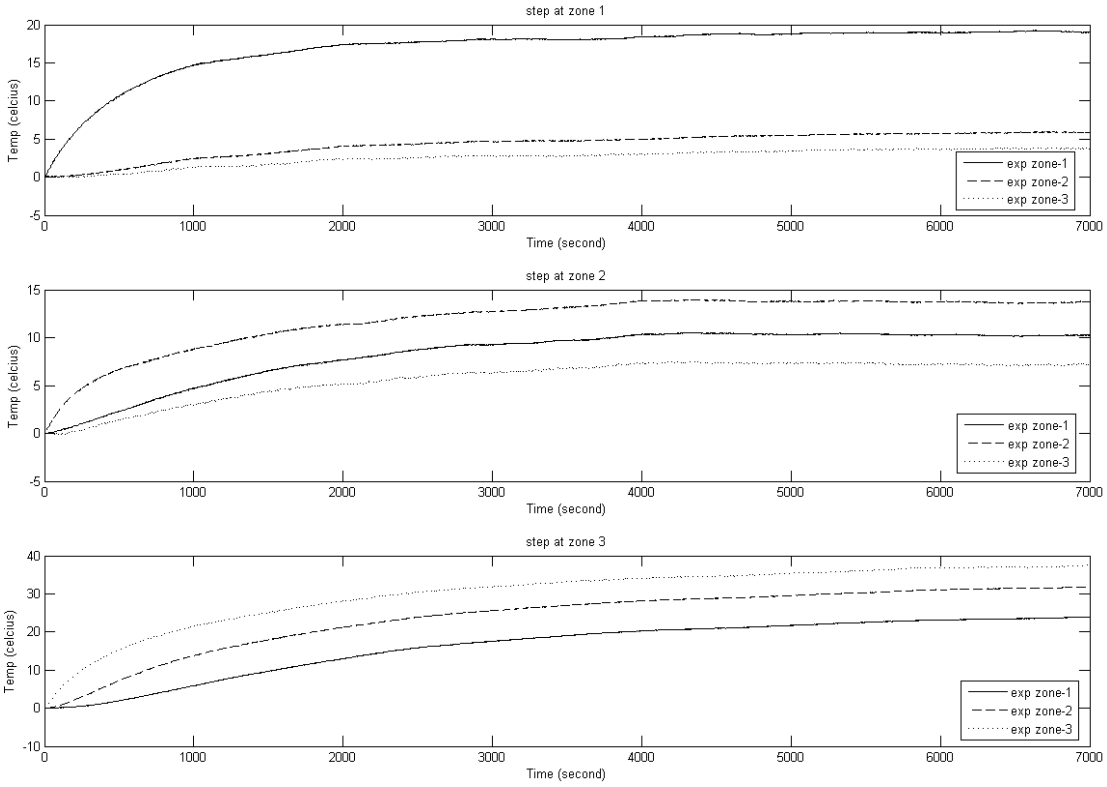

Figure 4-4: Step response of bake plate

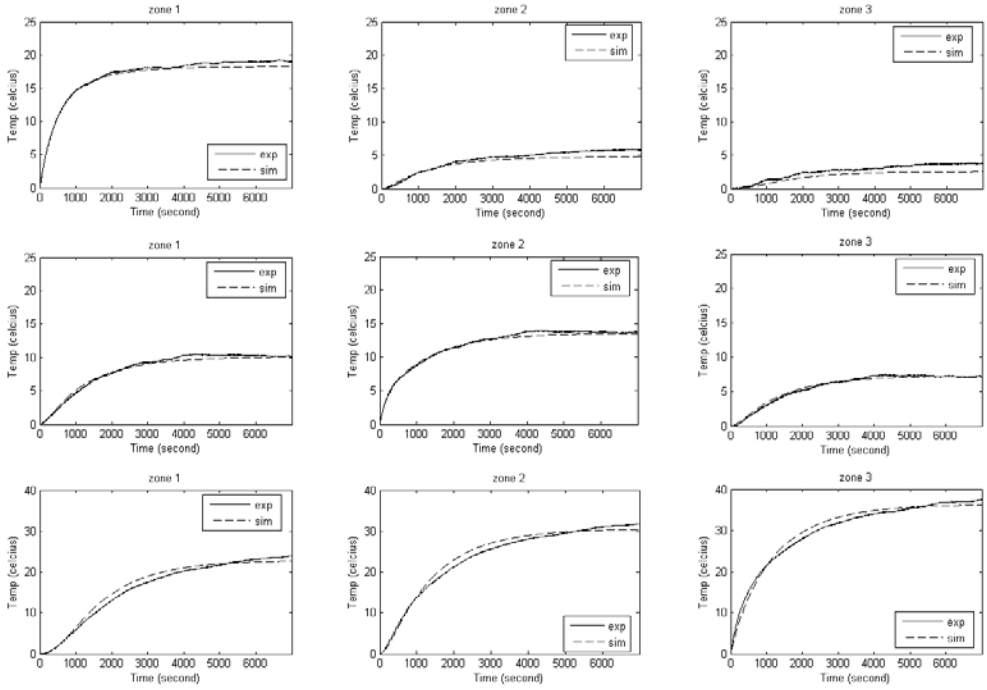

Figure 4-5: Comparison of simulation and experimental result for bake plate model. From top to bottom, step input applied at zone-1, zone-2, and zone-3

the values of bake plate parameters :

$$C_1 = 190.21J/K \qquad C_2 = 515.03J/K \qquad C_3 = 557.84J/K$$

$$r_1 = 8.15K/W \qquad r_2 = 3.12K/W \qquad r_3 = 1.27K/W$$

$$r_{12} = 2.75K/W \qquad r_{23} = 0.58K/W$$

Step response comparison between model simulation and experiment is shown in Figure 4-5 which shows that the model is acceptable.

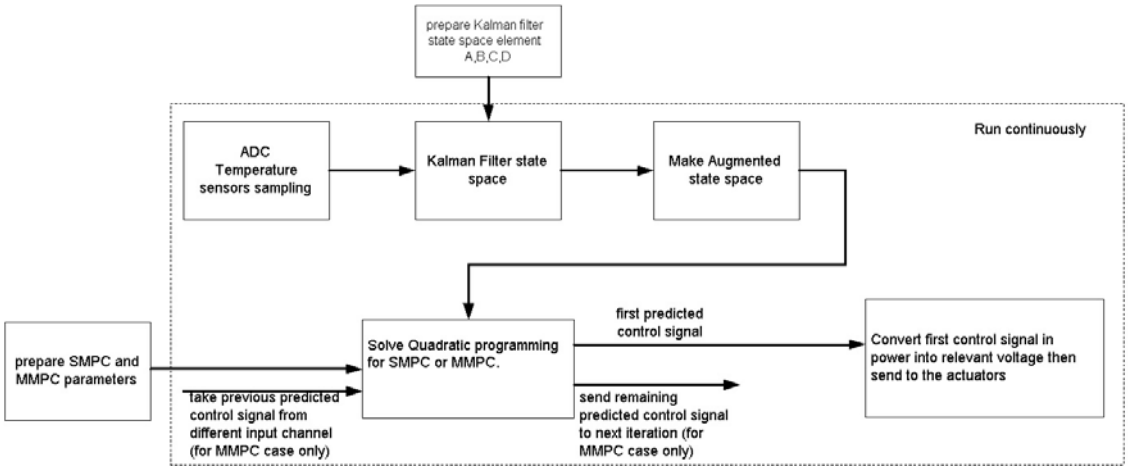

Figure 4-6: Diagram of close-loop experiment

The experimental setup for close loop experiment still using the same setup with open loop experiment (see Figure 4-3). However, now the MPC controller is working to maintain bake plate temperatures at set point automatically. Controller design and interface for the experiment are conducted in LabVIEW environment. Since noise is always present in real system, therefore kalman filter is used to get the true states. Diagram of experiment with kalman filter is shown in Figure 4-6. SMPC updates all input channels simultaneously, therefore every predicted control signal contains m inputs. However, MMPC updates one channel at a time so that every predicted control signal contains only one input which belong to different channel periodically $\sigma(k) = (k \bmod m) + 1$, where m is number of inputs.

4.3 Result and Discussion

In this section we show and compare the performance of MMPC and SMPC controllers to maintain temperature at set point 90^oC after wafer is dropped on top of the plate. The sampling time $Tb = 0.4s$ is our base period. MMPC sample and updates input one channel at a time at this base period, whilst SMPC also sample at base period but update all the inputs simultaneously at frame period $Tf = m \times Tb = 1.2s$, m is number of input.

Depending on thermal process, the recipe baking time can be less than four minutes and the temperature should recover within four minutes. It is also important to limit overshoot under 0.2^oC to avoid over evaporation. The experimental result of unconstrained SMPC and MMPC is shown in Figure 1-1. From this figure we can see clearly that MMPC recovers faster than SMPC after temperature drop due to wafer placement. From the control signals, it can be seen that MMPC has higher peak in shorter duration. After temperature drop MMPC temperature response had returned to 90^oC by 4 minutes and the overshoot is less than 0.2^oC for all three zones.

It can be seen that MMPC could reject the disturbance faster than SMPC. In this experiment, both the SMPC and MMPC were designed by optimizing the *same* cost function, only the admissible control law differs. To be more specific, the SMPC measured the temperature at $1.2s$ interval (at $t = 172.4s,\ 173.6s$ and $174.8s$ as marked by 'o' in Figure 3-3) while the MMPC measured the temperatures 3 times faster ($m = 3$) at $0.4s$ interval (at $t = 172.4s,\ 173.6s,\ \ldots$ marked by '*' in Figure 3-3). As a result, the

MMPC acquired more information than SMPC – a key reason for its better performance. In both cases, the zero-order-hold for the control signal were $1.2s$, the control horizons were $N_u = 5$ and the weights were $q = \begin{bmatrix} 0.01 & 0 & 0 \\ 0 & 0.1 & 0 \\ 0 & 0 & 0.2 \end{bmatrix}$, $r = 1$. As can be seen in Figure 3-3, the SMPC updates the three control signals simultaneously at interval of $1.2s$, i.e., at $t = 172.4s,\ 173.6s$ and $174.8s$ as indicated by the dashed lines in the figure. In comparison, MMPC also updates the control signal at $1.2s$ interval, but in a multiplex fashion, i.e., control signal 1 at $t = 172.4s,\ 173.6s$ and $174.8s$; control signal 2 at $t = 172.8s,\ 174s$ and $175.2s$; control signal 3 at $t = 173.2s,\ 174.4s$ and $175.6s$.

In our experiment, for safety reason we limit input voltage to $2.5V$ for every zone. Furthermore, for this specific experiment, none of the control signals exceed those constraints. However, MMPC will give more benefit when constraints are involved because computation becomes more complex.

We have conducted another experiment with constraints involved. We set the constraints values $u_1\,\min = u_2\,\min = u_3\,\min = 0V$ and $u_1\,\max = 0.95V$, $u_2\,\max = 0.76V$, and $u_3\,\max = 1.17V$ with the same weights and same horizon as unconstrained case. The experimental result is shown in Figure 4-7. We can see that control signals never exceed the constraints even though no saturator is used. When input constraints are considered in MPC control signal computation, controller will bound its action to neither lower than minimum constraints nor bigger than maximum constraints. In Figure 4-7 we can see that MMPC performance is similar with SMPC. As expected, these tight constraints

limit the advantage of MMPC over SMPC. However, MMPC performance is never worse than SMPC even in tight constraints.

4.3.1 Tuning MPC Parameters

Horizon selection is important in the implementation of MPC, because it will affect computation time needed to perform optimization especially control horizon. Wider horizon will expand the G matrix which eventually will add to the number of variables needed to be solved and therefore higher computational burden. Furthermore, wide horizon is not necessary since we are actually using infinite horizon formulation in our MPC cost function. In this experiment we choose prediction horizon value the same with control horizon $N2 = N_u = N = 5$ with assumption that in the constrained MPC, after 5 steps, the states will be more likely to enter maximum admissible set which will ensure the stability. From our observations, we have found that the time at which the disturbance occurs does not affect MPC controller performance. This happened because we are using fast sampling time.

Increasing input weight will make input increment Δu has bigger impact on cost function. As a result, controller will try to avoid large fluctuation in input and control signal becomes less responsive so that the bake plate temperature reaches set point in longer time. We have conducted experiments for different values of input weight as shown in Figure 4-8. From the pictures we can see that decreasing input weight will lead to faster response but higher overshoot. In this experiment, it is required for the

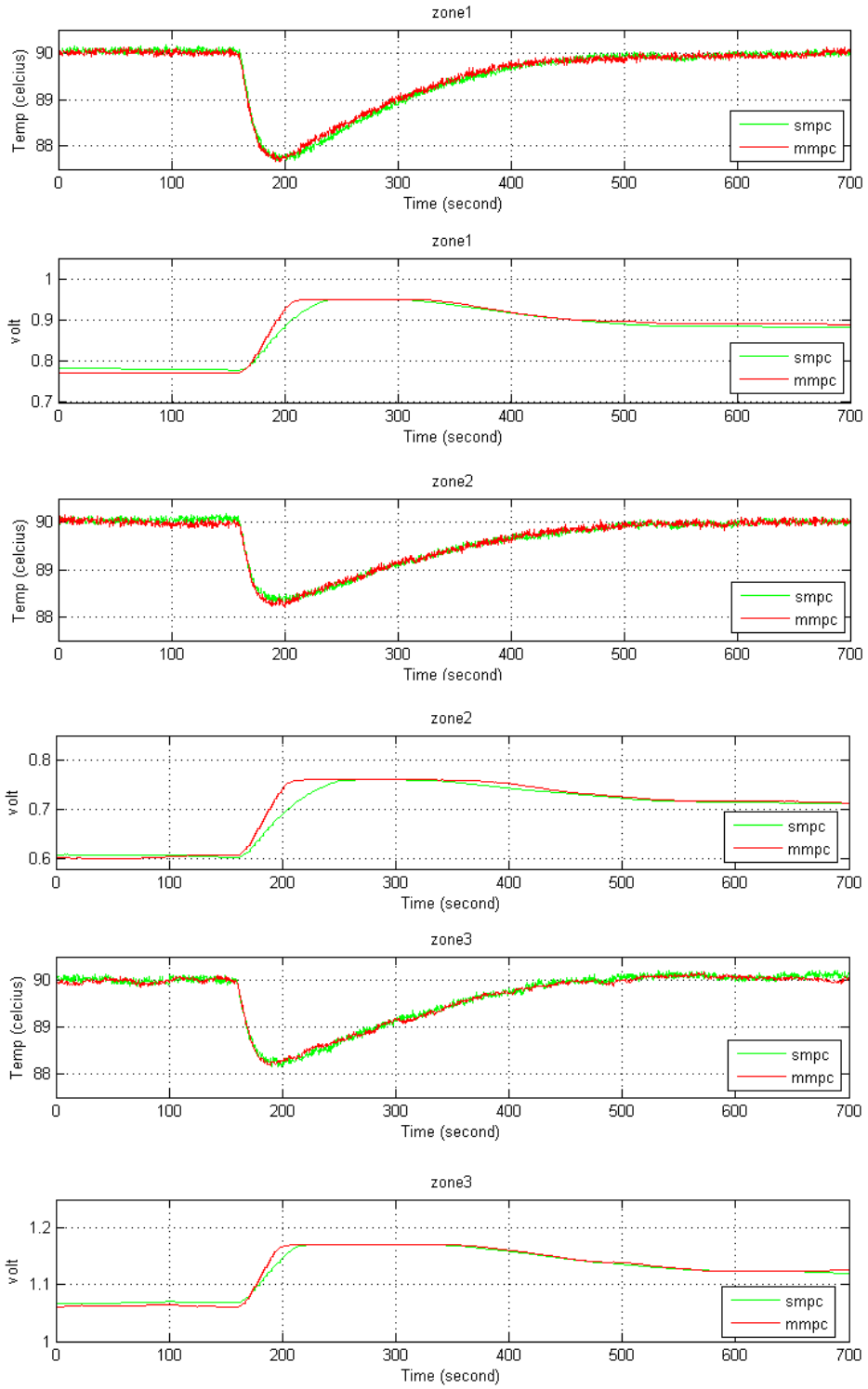

Figure 4-7: Experimental result of SMPC and MMPC for constrained case

temperature of all zones to be uniform and settle at the same time to avoid overbake in some of the zones. We should also limit the overshoot not to be bigger than 0.2^oC. Therefore, the tuning was directed to meet these requirements.

4.3.2 White Noise

White noise is a theoretical entity with flat power spectral and zero correlation. However, in real situation random signal with very small correlation like white noise is always present. In our experiment, white noise could come from fluctuating ambient air temperature. Since white noise is random signal, even though we use augmented state which contains component $x_k - x_{k-1}$, unlike constant disturbance, the net disturbance in steady state is not zero. In this experiment we use kalman filter to return the true states from disturbed measurement.

From our observation, we have found that SMPC can handle white noise well as it can still reach set point and stable. However, MMPC is badly affected as control signals keep oscillating with no clear pattern and plant becomes unstable as can be seen in Figure 4-9 which shows experimental result when controller takes and composes full states from noise distorted output measurements (temperatures) without kalman filter. This related to robustness of MMPC which is not investigated further in this thesis.

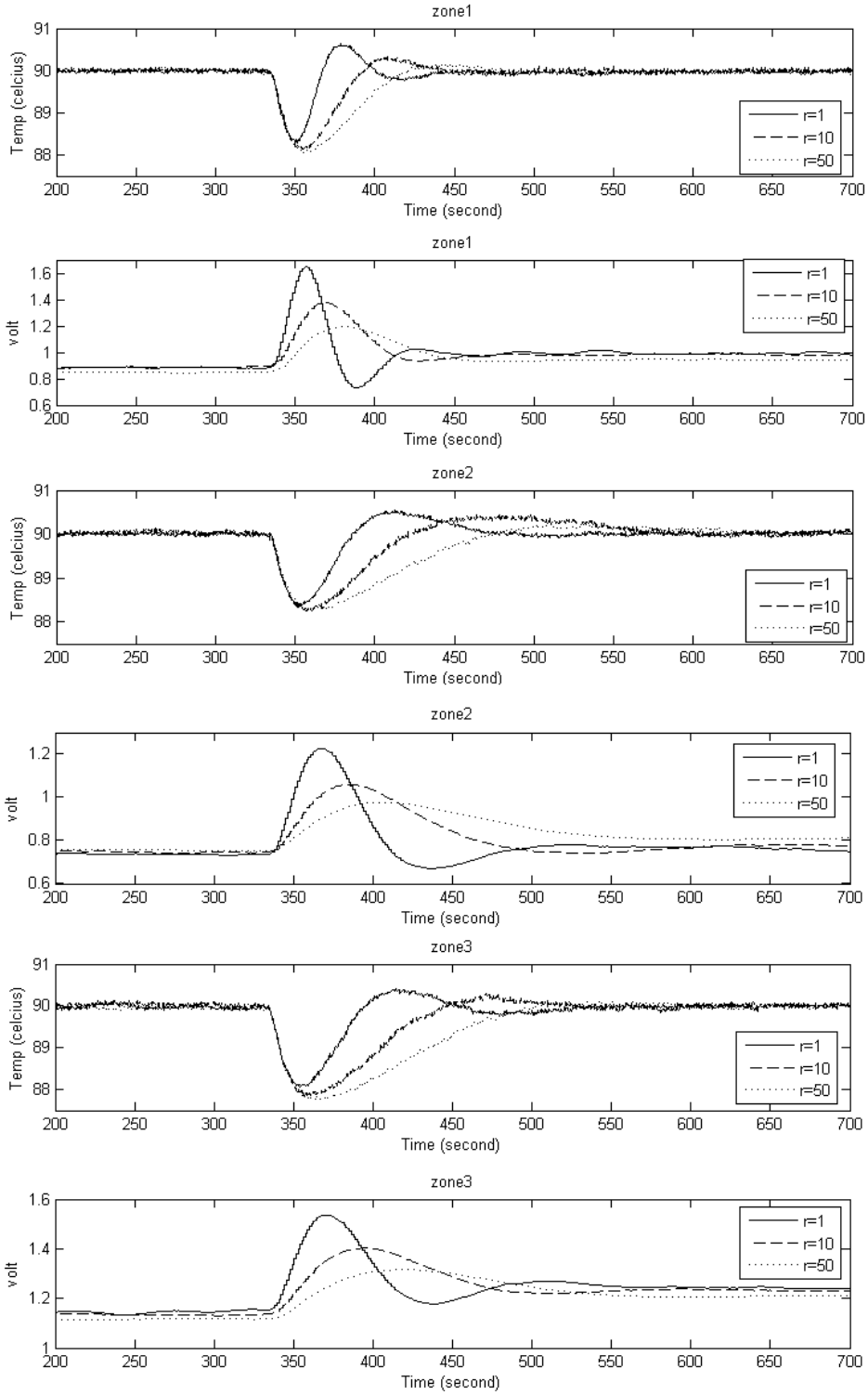

Figure 4-8: Experimental result of MMPC with different input weight r

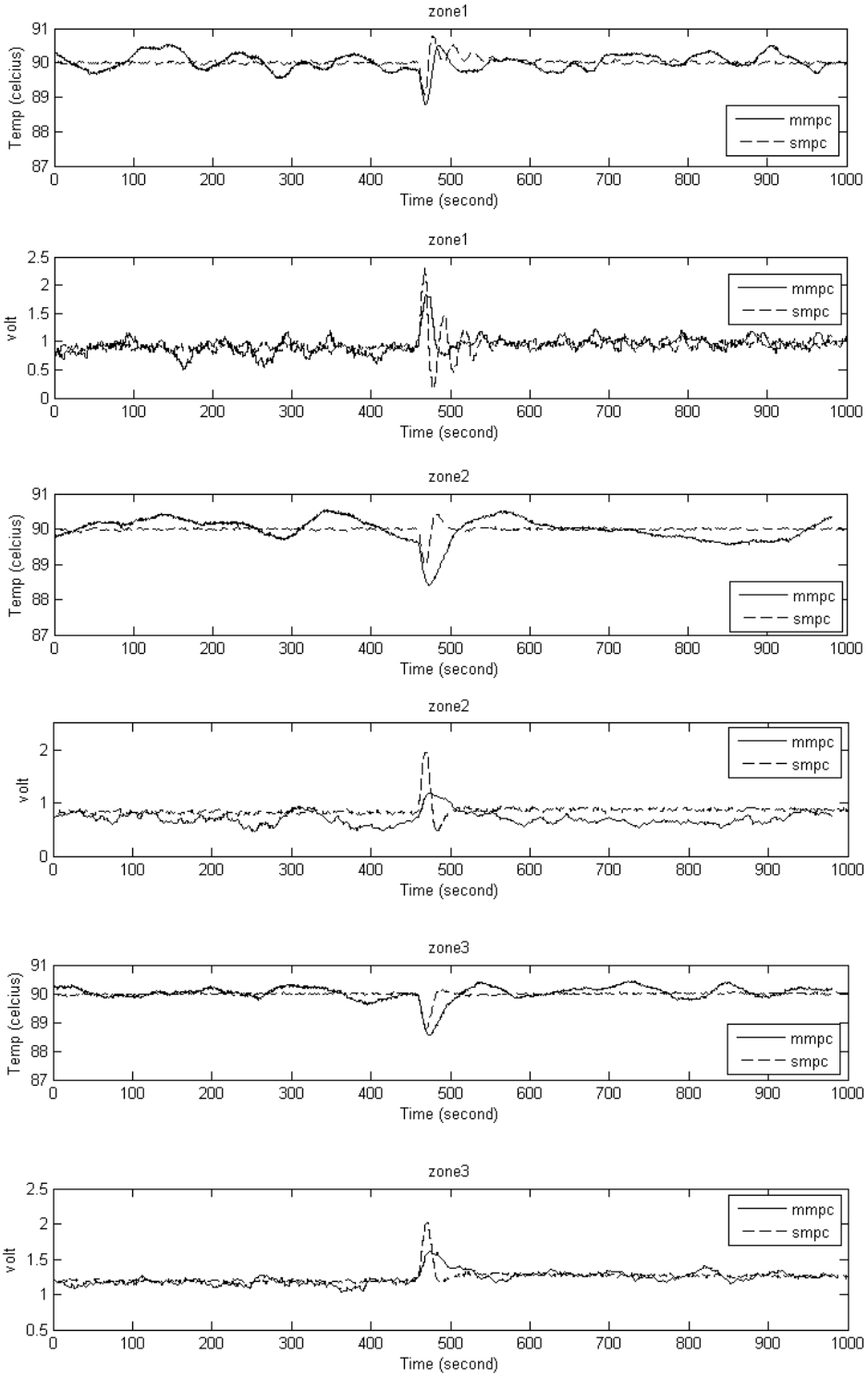

Figure 4-9: Experimental result of SMPC and MMPC when states taken directly from distorted measurements

Chapter 5

Conclusions and Recommendations

5.1 Conclusions

Multiplexed MPC has been demonstrated experimentally on a multi-zone bake plate application. MMPC can respond and recover faster than conventional MPC when disturbance takes place. This result is important for semiconductor wafer baking process because temperature non-uniformity will affect critical dimension (CD) of the wafer. With control horizon $N_u = 5$, conventional MPC need to optimize $m \times N_u = 15$ variables every sampling time whereas MMPC only need to optimize 5 which means computational burden for MMPC is a third of conventional MPC. This computational advantage of MMPC becomes even more significant when constraints are considered and with increasing number of zones and control horizon. For example, consider a 49-zone bake plate with $N_u = 5$. MMPC would have to solve an optimization problem with only 5 variables

whereas SMPC would have to solve an optimization problem of $49 \times 5 = 245$ variables.

5.2 Recommendations for Further Study

This thesis has showed that multiplexed MPC can work in real application. However, since MMPC is a novel technique, a lot of things can be developed to further increase its benefit on specific application especially for temperature uniformity control in wafer processing. Here we will give some ideas for future investigation:

- There are many variations we can do to the updating pattern in MMPC. For example, updating can be done on subset of inputs instead of single input or different update frequency for different inputs. We can also try to investigate proper updating interval to get better compromise between computation complexity and control performance. The effect of updating variation on controller performance could be interesting topics for further research.

- The nominal stability for MMPC has been proved in (Ling *et al.*, 2006). However, in real practice, modeling error would always exist and disturbances are inevitable. As we have found before, MMPC is not as robust as SMPC in the presence of white noise. Therefore, more thorough analysis on MMPC scheme robustness is very important topic for further research. A recent work by Richards *et al.* (2007) extended the multiplexed MPC with guaranteed robustness under uncertain but bounded disturbance. It is a very initial study, and further analysis needs to be

done. Our desire is to make it robust without adding to computation complexity.

- When wafer is dropped on top of the plate, it will be too late for any feedback controller to sense the disturbance and maintains bake plate temperature uniformity. Ho *et al.* (2002) and Tay *et al.* (2001) have introduced optimal feedforward control to compensate disturbance caused by cold wafer placement. While most of the temperature drop will be compensated by feedforward control, PID feedback control will take care the rest of error. Similar feedforward control with MMPC feedback control could improve recovery time and reduce the temperature drop.

- Since what important is to get good wafer thickness uniformity, it is advantageous to control its thickness directly rather than the temperature of bake plate. It is often that non-uniform temperature distribution across the wafer is needed to give good uniform wafer thickness in the endpoint. In (Lee *et al.*, 2002), various sites on wafer are made to follow predefined thickness trajectory to reduce wafer thickness non uniformity to less than 1nm at endpoint. This was realized by manipulating temperature of the bake plate using traditional MPC. MMPC scheme we have discussed here can be considered as a substitution for traditional MPC. MMPC's better recovery time characteristic compare to traditional MPC can be a benefit.

Bibliography

Bittanti, S. and J. C. Willems (1991). The periodic riccati equation. Springer-Verlag.

Bitmead, R. R., M. Gevers, and V. Wertz (1990). Adaptive Optimal Control: The Thinking Man's GPC. Englewood Cliffs, NJ: Prentice Hall.

Blanchini (1999). Set invariance in control. *Automatica* **35**(11),1747-1767.

Box, G. and A. Luceno (1997). Statistical Control by Monitoring and Feedback Adjustment. Wiley.

Cain, J. P., P. Naulleau and C. J. Spanos (2005). Critical dimension sensitivity to post-exposure bake temperature variation in euv photoresists. *Proc. SPIE* 5751, 1092-1100.

Camacho, E., F. and C. Bordons (2004). Model Predictive Control. Springer.

S. A. Campbell (1996). The Science and Engineering of Microelectronic Fabrication. London, U.K.: Oxford Univ. Press.

Edgar, T. P., S. W. Butler, W. J. Campbel, C. Pfeiffer, C. Bode, S. B. Hwang, K. S. Balakrishnan and J. Han (2000). Automatic control in microelectronics manufacturing: practices, challenges, and possibilities. *Automatica* **36**(11), 1567-1603.

El-Awady, K., C. Schaper and T. Kailath (1999). Control of spatial and transient temperature trajectories for photoresist processing. *J. Vacuum Sci. Technol. B.*

Franssila, S. 2004. Introduction to Microfabrication. Wiley.

Hamilton, S. (2003). Intel research expands moore's law. *Computer* **36**(1), 31-40.

Ho, W. K., A. Tay and C. D. Schaper (2000). Optimal Predictive Control with Constraints for Processing of Semiconductor Wafers on Bake Plates. *IEEE Transactions on Semiconductor Manufacturing* **13**(1), 88-96.

Ho, W. K., A. Tay, M. Chen, and C. M. Kiew (2007). Optimal Feed-Forward Control for Multizone Baking in Microlithography. *Ind. Eng. Chem. Res* **46**, 3623-3628.

International Technology Roadmap for Semiconductors, SIA (2005).

Kim, H. W., H. R. Lee, K. M. Kim, S. Y. Lee, B. C. Kim, S. H. Oh, S. G. Woo, H. K. Cho and W. S. Han (2004). Comprehensive analysis of sources of total cd variation in ArF resist perspective. *Proc. SPIE* **5376**, 254-265.

Lee, L. K., C. D. Schaper and W. K. Ho (2002). Real-Time Predictive Control of Photoresist Film Thickness Uniformity. *IEEE Transactions on Semiconductor Manufacturing* **15**(1), 51-59.

Li, T. L. (2001). Simulation of the post exposure bake process of chemically amplified resists by reaction diffusion equations. *Journal of Computational Physics* **173**, 348C363.

Ling, K. V., J. M. Maciejowski, and B. F. Wu (2005). Multiplexed Model Predictive Control. *16th IFAC World Congress,* Prague.

Ling, K. V., J. M. Maciejowski, and B. F. Wu (2006). Multiplexed Model Predictive Control. *Technical report Cambridge University Engineering Dept. CUED/FINGFENG/ TR561.*

Ling, K. V., J. M. Maciejowski, B. F. Wu (2008). Further Analysis of Multiplexed MPC and a Comparative Study. *ICARCV.*

Maciejowski, J. M. (2002). Predictive Control with Constraint. Harlow UK, Prentice Hall.

Miyagi, D., A. Saitou, N. Takahashi, N. Uchida and K. Ozaki (2006). Improvement of zone control induction heating equipment for high-speed processing of semiconductor devices. *IEEE Transactions on Magnetics* **42**(2), 292-294.

Moynes, J. (2006). A methodology for ROI analysis of run-to-run control solutions. *IFAC Workshop on Advanced Process Control for Semiconductor Manufacturing.*

Muske, K. R. and J. B. Rawlings (1993a). Linear Model Predictive Control of Unstable Processes. *Journal of Process Control* **3**(2), 85-96.

Muske, K. R and J. B. Rawlings (1993b). Model Predictive Control with Linear Models. *American Institute of Chemical Engineers Journal* **39**(2), 262-287.

Muske, K. R (1995). Linear Model Predictive Control of Chemical Process. Ph.D. dissertation, University of Texas at Austin.

Pawlowski, G (1997). Acetal-based DUV photoresists for sub-quarter micron lithography. *Semiconductor FABTECH, Lithography*, 6th ed.

Postnikov, S., S. Hector, C. Garza, R. Peters, and V. Ivin (2003). Critical dimension control in optical lithography. *Microelectronic Engineering* **69**(2-4), 452-458.

Raptis, I. (2001). Resist lithographic performance enhancement based on solvent removal measurements by optical interferometry. *Japanese Journal of Applied Physics* **40**(9A), 5310-5311.

Richards, A. G., K. V. Ling, and J. M. Maciejowski (2007). Robust Multiplexed model predictive control. *European Control Conference*.

Roberts, P. D. (2000). A brief overview of model predictive control. *IEEE Seminar on Practical Experiences with Predictive Control*.

Schaper, C. D., M. Moslehi, K. Saraswat, and T. Kailath (1994). Modelling, identification, and control of rapid thermal processing systems. *J. Electrochemical Soc.* **141**(11), 3200-3209.

Schaper, C. D., K. El-Awady, and A. Tay (1999). Spatially programmable temperature control and measurement for chemically amplified photoresist processing. *Proc. SPIE* **3882**, 74-79.

Sturtevant, J., S. Holmes, T. VanKessel, P. Hobbs, J. Shaw and R. Jackson (1993). Post exposure bake as a process-control parameter for chemically-amplified photoresist. *Proc. SPIE* **1926**, 106-114.

Tay, A., W. K. Ho and Y. P. Poh (2001). Minimum time control of conductive heating systems for microelectronics processing. *IEEE Transactions on Semiconductor Manufacturing* **14**(4), 381-386.

Tay, A., W. K. Ho, C. D. Schaper and L. L. Lee (2004). Constraint Feedforward Control for Thermal Processing of Quartz Photomasks in Microelectronics Manufacturing. *Journal of Process Control* **14**(1), 31-34.

Watlow (1995). SCR power control. The watlow educational series book six.

Wu, B. F. (2005). Various Ways to Compute Periodic Gains for Multiplexed MPC. A study report.

Appendix A

Derivation of the equivalent LQ Problem for SMPC

This section will briefly explain how to change cost function for SMPC from base period into frame period in order to make fair comparison between SMPC and MMPC.

First, denote $\bar{Q} = diag(q, ..., q)$ and

$$\begin{aligned} \bar{x}_{k+jm} &= \begin{bmatrix} x_{k+jm} \\ x_{k+jm+1} \\ \vdots \\ x_{k+jm+m-1} \end{bmatrix} = \begin{bmatrix} I \\ A \\ \vdots \\ A^{m-1} \end{bmatrix} x_{k+jm} + \begin{bmatrix} 0 \\ B \\ \vdots \\ A^{m-2}B \end{bmatrix} \Delta u_{k+jm} \\ &= \bar{A}x_{k+jm} + \bar{B}\Delta u_{k+jm} \end{aligned}$$

Next, perform the following manipulations to the SMPC cost function

$$\begin{aligned}
J_{SMPC} &= \sum_{i=0}^{\infty} \|x_{k+i}\|_q^2 + \|\Delta u_{k+i}\|_{\bar{R}}^2 \\
&= \sum_{j=0}^{\infty} \sum_{i=0}^{m-1} (\|x_{k+jm+i}\|_q^2 + \|\Delta u_{k+jm+i}\|_{\bar{R}}^2) \\
&= \sum_{j=0}^{\infty} \|\bar{x}_{k+jm}\|_{\bar{Q}}^2 + \|\Delta u_{k+jm}\|_{\bar{R}}^2 \\
&= \sum_{j=0}^{\infty} \left\|\bar{A}x_{k+jm} + \bar{B}\Delta u_{k+jm}\right\|_{\bar{Q}}^2 + \|\Delta u_{k+jm}\|_{\bar{R}}^2 \\
&= \sum_{j=0}^{\infty} \|x_{k+jm}\|_{\bar{A}^T\bar{Q}\bar{A}}^2 + \|\Delta u_{k+jm}\|_{\bar{B}^T\bar{Q}\bar{B}+\bar{R}}^2 + 2x_{k+jm}^T \bar{A}^T\bar{Q}\bar{B}\Delta u_{k+jm}
\end{aligned}$$

and note that

$$x_{k+(j+1)m} = A^m x_{k+jm} + A^{m-1}B\Delta u_{k+jm}$$

Appendix B

Derivation of the Stabilizing Terminal Weight for MMPC

In this section, we show how the terminal weight for MMPC and a stabilizing feedback gain can be computed. The solution to the unconstrained infinite horizon periodic optimal control problem is well studied (Bittanti *et al.*, 1991). The optimal control problem is

$$\Delta\tilde{u}_k = -(B_{\sigma(k)}^T P_{k+1} B_{\sigma(k)} + r)^{-1} B_{\sigma(k)}^T P_{k+1} A x_k = -K_{\sigma(k)} x_k \tag{B.1}$$

where $P_{(.)}$ is the backward solution of the following discrete time periodic riccati equation (DPRE)

$$P_k = A^T P_{k+1} A - A^T P_{k+1} B_{\sigma(k)} (B_{\sigma(k)}^T P_{k+1} B_{\sigma(k)} + r)^{-1} B_{\sigma(k)}^T P_{k+1} A + q \tag{B.2}$$

In general, the solution $P_{(.)}$ does not have to be periodic, unless a suitable final condition is chosen. Such a final condition is referred to as a periodic generator. Bittanti *et al.* (1988,1991) discuss some conditions for the existence and uniqueness of solution B.2 and provide algorithms for finding it; note that this solution can be pre-computed off-line.

Here, we follow the time-invariant approach as suggested in (Bittanti *et al.*, 1991). We begin with the following infinite horizon control problem for the periodic system of 3.8. The cost function is

$$J = \sum_{i=0}^{\infty} \|x_{k+i}\|_q^2 + \|\Delta\tilde{u}_{k+i}\|_r^2 \tag{B.3}$$

The cost function can be re-written as

$$\begin{aligned} J &= \sum_{j=0}^{\infty}\sum_{i=0}^{m-1} \|x_{k+jm+i}\|_q^2 + \|\Delta\tilde{u}_{k+jm+i}\|_r^2 \\ &= \sum_{j=0}^{\infty} \|\bar{x}_{k+jm}\|_{\bar{q}}^2 + \|\Delta\tilde{u}_{k+jm}\|_{\bar{r}}^2 \end{aligned}$$

where $\bar{q} = diag(q,\ldots,q)$, $\bar{r} = diag(r,\ldots,r)$,

$$\bar{x}_k = \begin{bmatrix} x_k \\ x_{k+1} \\ \vdots \\ x_{k+m-1} \end{bmatrix}, \qquad \Delta\bar{u}_k = \begin{bmatrix} \Delta\tilde{u}_k \\ \Delta\tilde{u}_{k+1} \\ \vdots \\ \Delta\tilde{u}_{k+m-1} \end{bmatrix}$$

The "lifted" signals $\bar{x}_k$ and $\Delta\bar{u}_k$ can be constructed as (Wu, 2005)

$$\begin{aligned}\bar{x}_k &= \begin{bmatrix} I \\ A \\ A^2 \\ \vdots \\ A^{m-1} \end{bmatrix} x_k + \begin{bmatrix} 0 & \cdots & \cdots & 0 \\ B_{\sigma(k)} & & \vdots & \\ AB_{\sigma(k)} & B_{\sigma(k+1)} & & \vdots \\ \vdots & & \ddots & \vdots \\ A^{m-2}B_{\sigma(k)} & & B_{\sigma(k+m-2)} & 0 \end{bmatrix} \Delta\bar{u}_k \\ &= \bar{A}x_k + \bar{B}_{\sigma(k)}\Delta\bar{u}_k\end{aligned}$$

so that

$$\begin{aligned}J &= \sum_{j=0}^{\infty} \|\bar{x}_{k+jm}\|_{\bar{q}}^2 + \|\Delta\bar{u}_{k+jm}\|_{\bar{r}}^2 \\ &= \sum_{j=0}^{\infty} \left\|\bar{A}x_{k+jm} + \bar{B}_{\sigma(k)}\Delta\bar{u}_{k+jm}\right\|_{\bar{q}}^2 + \|\Delta\bar{u}_{k+jm}\|_{\bar{r}}^2 \\ &= \sum_{j=0}^{\infty} \|x_{k+jm}\|_{\bar{A}^T\bar{q}\bar{A}}^2 + \|\Delta\bar{u}_{k+jm}\|_{\bar{B}_{\sigma(k)}^T\bar{q}\bar{B}_{\sigma(k)}+\bar{r}}^2 + 2x_{k+jm}^T\bar{A}^T\bar{q}\bar{B}_{\sigma(k)}\Delta\bar{u}_{k+jm}\end{aligned}$$

subject to $x_{k+m} = A^m x_k + \tilde{B}_{\sigma(k)}\Delta\bar{u}_k$ where

$$\tilde{B}_{\sigma(k)} = \begin{bmatrix} A^{m-1}B_{\sigma(k)} & \cdots & B_{\sigma(k+m-1)} \end{bmatrix}$$

This is a standard infinite horizon optimal control problem with a cross term.

Let

$$\begin{aligned} Q &= \bar{A}^T \bar{q} \bar{A} - S^T R^{-1} S \\ R &= \bar{B}_{\sigma(k)}^T \bar{q} \bar{B}_{\sigma(k)} + \bar{r} \\ S &= \bar{A}^T \bar{q} \bar{B}_{\sigma(k)} \\ \tilde{A} &= A^m - R^{-1} S^T \\ v_k &= \Delta \bar{u}_k + R^{-1} S^T x_k \end{aligned}$$

The optimal control problem is equivalent to minimizing the following cost function

$$J = \sum_{j=0}^{\infty} \|x_{k+jm}\|_Q^2 + \|v_{k+jm}\|_R^2$$

subject to $x_{k+m} = \tilde{A} x_k + \tilde{B}_{\sigma(k)} v_k$

The optimal control law is

$$\Delta \bar{u}_k = -(\tilde{K} + R^{-1} S^T) x_k = -\bar{K}_{\sigma(k)} x_k$$

where

$$\tilde{K} = (\tilde{B}_{\sigma(k)} P_{\sigma(k)} \tilde{B}_{\sigma(k)} + R)^{-1} \tilde{B}_{\sigma(k)}^T P_{\sigma(k)} \tilde{A}$$

and $P_{\sigma(k)}$ satisfies the following ARE (Algebraic Riccati equation)

$$P_{\sigma(k)} = Q + \tilde{A}^T P_{\sigma(k)} \tilde{A} - \tilde{A}^T P_{\sigma(k)} \tilde{B}_{\sigma(k)} (\tilde{B}_{\sigma(k)}^T P_{\sigma(k)} \tilde{B}_{\sigma(k)} + R)^{-1} \tilde{B}_{\sigma(k)}^T P_{\sigma(k)} \tilde{A}$$

The infinite horizon optimal cost is

$$J_{\sigma(k)} = x_k^T P_{\sigma(k)} x_k$$

Once the value of $\sigma(k)$ is chosen, the terminal weight can be calculated as shown above. Bittanti *et al.* (1991) discussed conditions when the time-invariant re-formulation of a periodic control problem coincides with the SPPS solution.